19

Planetary geomorphology

19.1 Approaches to planetary geomorphology

We conclude this survey of global geomorphology by expanding our horizons to the earth-like planetary bodies of the Solar System. By earth-like we mean those planets and large moons composed of a solid crust on which landforms can develop and be preserved. The term 'terrestrial' is reserved to designate those features actually occurring on the Earth. The interpretation of surface planetary features is carried out in part by analogy with terrestrial landforms, although some planetary landforms appear to have no terrestrial analogues. Many planetary bodies, such as the Earth's moon, retain landscape features formed very early in their history, and their study provides a context in which to interpret the long-term history of the Earth's surface. Moreover, comparative planetary geomorphology gives a basis for understanding how our Earth alone among the planets and moons of the Solar System came to develop its apparently uniquely complex surface form.

It is possible in this chapter to give only the very briefest outline of the exciting findings that have come from the various planetary orbiter and lander missions of the USA and the USSR. This is a fast-moving field of research, and although spectacular landforms have already been revealed by the initial examination of the mass of imagery returned to Earth, further more detailed analyses will no doubt provide a much fuller picture of the development of planetary surfaces.

Some of the global properties of the inner planets which directly or indirectly influence the operation of geomorphic processes are listed in Table 19.1. The mean distance of the Sun influences the amount of solar energy available at the

Table 19.1 Properties of the inner planets

	EARTH	MOON	MARS	MERCURY	VENUS
Mean distance from the Sun (km × 10^6)	149.6	0.3844*	227.9	57.9	108.2
Period of revolution (Earth days)	365.26	27.32*	687	88	224.7
Rotation period (Earth days)	0.9983	27.32	1.026	59	243 retrograde
Equatorial diameter (km)	12 756	3476	6787	4880	12 104
Mass (Earth = 1)	1	0.01226	0.108	0.055	0.815
Density (kg m^{-3})	5500	3340	3900	5400	5200
Atmosphere (main components)	Nitrogen, oxygen	None	Carbon dioxide	None	Carbon dioxide
Atmosphere (minor components)	Carbon dioxide, noble gases	None	Noble gases, nitrogen	None	Noble gases; hydrochloric hydrofluoric and sulphuric acids
Mean temperature at surface (°C)	15	107 (day) -153 (night)	-23	305 (day) -170 (night)	480
Atmospheric pressure at surface (millibars)	1000	0	6	$<10^{-9}$	90 000
Surface gravity (Earth = 1)	1	0.16	0.38	0.37	0.88

* Relative to the Earth.
Source: Modified from B. Murray *et al.* (1981) *Earthlike Planets*. W. H. Freeman, San Francisco, Table 2.1 p. 28.

surface, and together with the rotational period and the nature of the atmosphere this largely controls the average and extreme temperatures experienced on planetary surfaces. Atmospheric pressure and temperature are two crucial variables which determine whether water can exist in its liquid state on a planet's surface, and consequently they determine the nature of chemical and physical weathering and the presence or absence of fluvial activity. Surface gravity is a significant factor in influencing atmospheric pressure and indirectly in controlling the existence and nature of aeolian activity; moreover, it directly affects the operation of mass movement processes. There are in fact complex interactions between several of these factors, and we will consider these further as we discuss the geomorphology of individual planetary bodies.

19.2 The Moon

Knowledge of the broad outlines of the Moon's surface features extends back to the time when human beings first looked heavenwards. Contrasts between light and dark areas are clearly visible with the naked eye and, following the observations by telescope pioneered by Galileo and others in the seventeenth century two major types of terrain were identified – the high albedo, heavily cratered uplands and the low albedo, smooth, lightly cratered lowlands, called **maria** (singular **mare**) because of their supposed resemblance to seas). The Ranger, Lunar Orbiter and Apollo programmes of the USA, together with a number of Soviet missions, have now provided an abundance of data on the Moon. Although many questions remain, we now have a fairly clear idea of the processes that have shaped the lunar surface and an approximate chronology for its development, based on the radiometric dating of rock samples returned to Earth.

Two major processes have fashioned the lunar landscape. One is **impact cratering**, which involves the transformation of the kinetic energy of an impacting object, or **bolide**, and the consequent formation of **impact craters** and associated features. Bolides can include comets and asteroids as well as meteorites. The second significant process is volcanic flooding. The maria are plains formed by extensive sheets of basaltic lava, erupted mainly between 3.9 and 3.1 Ga BP. Some 17 per cent of the surface is covered by lava plains, but by far the greater proportion of these occur on the near side of the Moon. The far side, which is always turned away

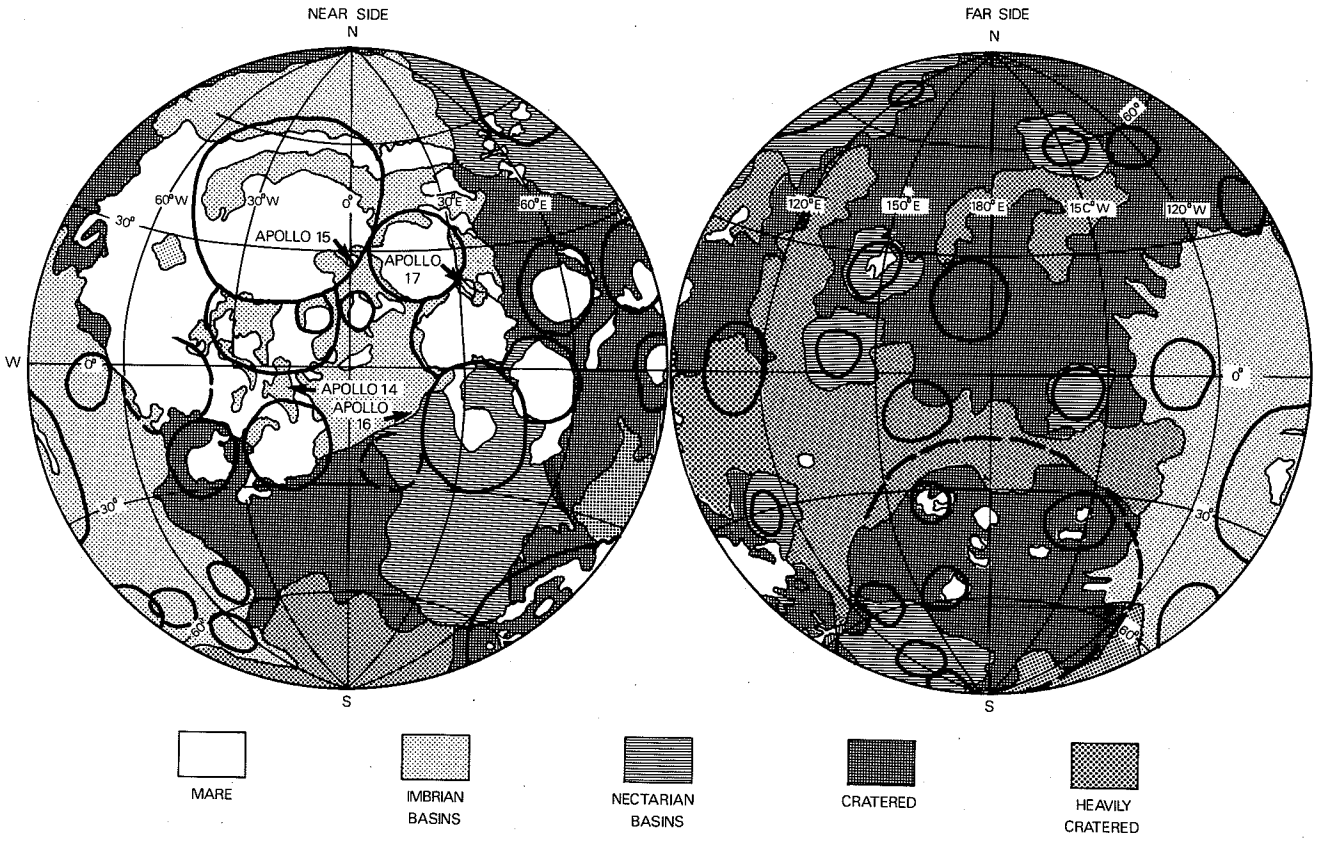

Fig. 19.1 Maps of the near side and far side of the Moon showing the major geological and morphological provinces. The location of the landing sites for Apollo missions 14–17 are also indicated. (After K. A. Howard et al. *(1974)* Reviews of Geophysics and Space Physics ***12***, *Fig. 14 p. 322. Copyright by the American Geophysical Union.)*

from the Earth because of gravitational interactions arising from irregularities in the form of the two bodies, is almost completely covered by moderately to heavily cratered terrain (Fig. 19.1).

19.2.1 Impact cratering

The Moon has experienced a history of bombardment extending back to its formation 4.6 Ga BP. Craters formed by bolide impacts range from microscopic forms up to huge circular basins, such as the Mare Imbrium, which have subsequently been flooded by lava. A small number of craters of probable non-impact origin have also been identified on the Moon and are thought to be associated with volcanic activity.

Impacts occur at tremendous velocities of up to 150 000 km h^{-1}. The instantaneous conversion of the enormous quantities of kinetic energy released into heat as the object penetrates the surface, explodes and vaporizes means that small objects can produce surprisingly large craters. For example a 50 t meteorite about 3 m across can form a crater 150 m in diameter. As the kinetic energy of a projectile is proportional to the square of its velocity, bolide size is less important than speed in determining the size of the crater formed.

At the simplest level, lunar craters can be classified according to their size and characteristic morphology into four categories. Microcraters (< 10 mm in diameter) are found on rocks and boulders, and bombardment by very small meteorites is probably important in fracturing rocks and producing the fine-grained lunar regolith. Small craters (10 mm to 15 km across) have a simple form lacking major structural features, whereas large craters (15 to 300 km across) are complex features and typically show evidence of modification by molten rock, either related to the original impact or associated with subsequent volcanic activity. Some contain one or more central peaks probably formed through the rebound of the crater floor after impact (Fig. 19.2).

In craters more than about 120 km across, a series of rings formed by uplifted masses of rock tends to replace the central peak. In very large craters (> 300 km across), usually termed **basins**, up to five rings may be found. Most lunar mountain chains are formed from these large circular structures and most large fracture systems are related to them. The Montes Apennines, which reach some 5 km above the lunar surface, in fact represent part of the outermost ring of the vast Imbrium Basin. The origin of these multi-ringed basins is uncertain, but probably involved adjustments of the lunar crust after the impact of very large bolides during the early stages of the Moon's history.

19.2.2 Volcanism and tectonics

Although now quiescent, volcanic activity has been active on the Moon in the past. Most was associated with the formation of large impact basins, all of which were created early in lunar history. The Orientale Basin is the most recent and this was formed about 3.9 Ga BP. Puncturing of the early-formed crust by large bolides exposed the partially molten interior and led to the eruption of lava flows which proceeded to fill the basins. Eruption of basalts appears to have continued for a considerable period after basin formation.

During the Apollo 15 mission to Hadley Rille, a sinuous channel cutting across the Mare Imbrium, individual lava flows up to 60 m thick were observed. The Hadley Rille itself is thought to be a massive collapsed lava tunnel, smaller versions of which are known from lava fields on Earth (Fig. 1.1). Some idea of lava thicknesses can be gained by measuring the rim heights of craters partially buried by lava and

Fig. 19.2 *View of the relatively young, 27 km diameter lunar crater Euler located in the south-west of the Mare Imbrium. A central peak can be seen in the centre of the crater, probably formed as a result of rebound of the crater floor after impact. The effects of impact are seen to extend well beyond the primary crater since in the Moon's low gravity field ejecta may travel for hundreds of kilometres before returning to the surface to form large numbers of much smaller secondary craters. The bright bands that can be seen radiating away from the crater (particularly towards the top left) are known as* ***crater rays****. They are typical features of relatively young craters and are probably composed of fine material ejected on impact, including highly reflective fused silica (glass) beads formed by the shock waves generated by the primary impact explosion. With age these bright rays become darker and less conspicuous probably as a consequence of burial by ejecta from later impact events or changes in the crystal structure of the silica beads brought about by the intense ultra-violet radiation which reaches the unshielded lunar surface. (Apollo 17 image, World Data Center A for Rockets and Satellites.)*

comparing these with their likely original heights. Such analyses indicate that basin lava thicknesses of 300 m are typical. In addition to rilles, other landforms associated with volcanic activity include lobate flow fronts on lava flows, low elevation shield volcanoes up to 15 km or so across, and domed-shaped hills, which although of less certain volcanic origin, may have been formed from lavas more viscous than those which cover the mare basins.

Data from seismographs on the lunar surface show that the current level of seismic activity on the Moon is minimal, being only about one-millionth of that on the Earth. The Moon has in fact experienced little tectonic activity over the past 3 Ga apart from crustal dislocations associated with impact events. Nevertheless, some tectonic structures have been recorded; for instance, graben are locally abundant and some mare ridges may not be of purely volcanic origin but rather true tectonic features associated with vertical movements within the sub-basin crust.

19.2.3 Surface materials and processes

Apart from forming craters, bolide impacts also create the lunar regolith. This is made up of rock particles detached from bedrock, ejecta and molten rock from impact events (the latter consisting largely of fused silica in the form of glass beads) and minor amounts of bolide fragments. The most effective bolide size for generating regolith is the range which forms craters – about 10–1500 m in diameter. Larger bolides are too infrequent to be significant, while smaller objects are rarely able to penetrate the existing regolith cover and thus create any additional regolith material. None the less, small meteorites, down to those of microscopic dimensions, which can reach the lunar surface in the absence of an atmosphere, do play a role in pitting the rock surface and smoothing features at the small scale. The effectiveness of this mechanism, however, is minimal in comparison with processes of terrestrial denudation. This is apparent from the preservation of 10 m high features on lava flows over 3 Ga old observed by Apollo astronauts. The consequences of bolide impacts are not confined to fragmentation of the

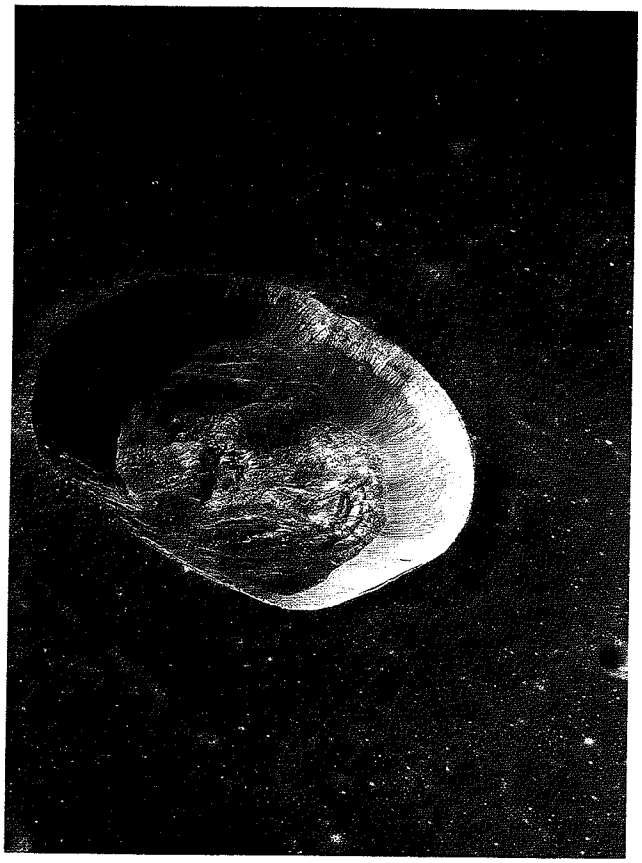

Fig. 19.3 *The 18 km diameter lunar crater Dawes showing clear evidence of mass movement in the form of extensive accumulations of debris on the crater floor. (Apollo 17 image, World Data Center A for Rockets and Satellites.)*

Fig. 19.4 *Boulder track on the slopes of the North Massif of the Moon near the Apollo 17 landing site. The track is nearly 1 km long and the largest boulders visible are about 5 m across. (Apollo 17 image, World Data Center A for Rockets and Satellites.)*

surface since the pressure and heat generated on impact is capable of fusing unconsolidated sediments together to form breccia.

In the absence of the transporting agents of water, wind and ice, movement of surface materials on the lunar surface (excluding the effects of bolide impacts and lava flows) is confined to mass movements. There is abundant evidence for such activity; slumping associated with impact events is indicated by the morphology of the terraced inner walls of large craters (Fig. 19.3) and tracks left by large boulders sliding down crater slopes have also been observed (Fig. 19.4). Landslides of unstable ejecta mantling crater wall slopes could be triggered by the seismic shocks generated by large bolide impacts, but downslope movement may also be precipitated by the subsequent impact of ejecta from such events. The scarcity of post-mare landslides, however, suggests that the occurrence of mass movement may have diminished after the early period of high cratering rates.

19.2.4 History of landscape development

The history of the lunar landscape has now been established in broad outline by calculating the density of cratering and the freshness of craters over different parts of the surface, and relating these variables to the radiometric dates provided from the Apollo lunar samples (Table 19.2). There are some uncertainties as to the accuracy of these dates (different radiometric techniques giving slightly different results) and there are also discrepancies between the various approaches taken to relate the density of cratering to the age of the surface. Nevertheless, the very low rate of modification of the lunar surface compared with the Earth means that we have a much clearer idea of its long-term geomorphic history.

After the formation of the Moon 4.6 Ga BP a process of differentiation of its constituents led to the formation of a crust which became sufficiently solidified by about 4.3 Ga BP to record impact events. Most of this very early Pre-Nectarian terrane (Table 19.2) is preserved as very subdued basins and craters on the far side of the Moon. Formation of the large lunar basins was concentrated between about 4.3 and 3.9 Ga BP and ended with the creation of the vast Imbrium Basin at the termination of the Nectarian System. Prior to the Apollo missions the lunar highlands were thought to be remnants of the earliest accretionary phase of the Moon's history when it was subject to continuous bombardment. Radiometrically dated Apollo samples, however, suggest a predominant age of around 4 Ga which indicates

Table 19.2 Chronology of landscape development on the Moon

TIME-STRATIGRAPHIC UNITS	AGE (Ga)	ROCK UNITS	EVENTS	NOTES
Copernican System		Few large craters	Tycho	Craters with bright rays and sharp features at all resolutions (e.g. Tycho, Aristarchus)
		Few large craters	Aristarchus	Craters with bright rays and sharp features but now subdued at metre resolutions (e.g. Copernicus)
			Copernicus	
		Few large craters	Eratosthenes	Craters with Copernican form but rays barely visible or absent
Eratosthenian System	3.2	Apollo 12 lavas		
	3.3	Apollo 15 lavas	Imbrium lavas	Few lavas with relatively fresh surfaces
	3.42	Luna 16 lavas		
		Mare lavas	Eruption of widespread lava sheets on near side: few eruptions on far side	Extensive piles of basaltic lava sheets with some intercalated impact crater ejects sheets
Imbrian System	3.6	Apollo 11 lavas		
	3.8	Apollo 17 lavas		
	3.9		Orientale Basin	
			Imbrium Basin	
Nectarian System			Crisium, Muscoviense, Humorum, Nectaris, Serenitatis, Smythii, Tranquillitatis, Nubium (Basins)	Numerous overlapping large impact craters and associated ejecta sheets together with large basin ejecta
	4.1			Any igneous activity at surface obscured by impact craters
Pre-Nectarian				
	4.6		Formation of Moon	Crystalline rocks formed by early igneous activity

Source: Modified from J. E. Guest and R. Greeley (1977) *Geology on the Moon*. Wykeham Publications, London, Fig. 1.5, p. 8.

that there was a period of frequent impacts by large bolides well after the initial accretionary phase.

This episode of intensive impact cratering is known as the **Late Heavy Bombardment**. The dating uncertainties already mentioned have led to a number of rather different interpretations of the details of this event. One suggestion is that the Late Heavy Bombardment represents the end of a 500 Ma period of continuous but declining impact activity. Another view is that there was a short-lived cataclysmic increase in the rate of bombardment around 4 Ga. Whatever the correct interpretation, evidence of the Late Heavy Bombardment on the Moon is of crucial importance as it provides a time scale for similar events which appear to have affected all the inner planets, and also possibly some of the more remote planetary bodies of the Solar System.

Infilling of the large lunar basins by lava flows occurred from about 3.8 to 3.2 Ga (Imbrian and Eratosthenian Systems). Geomorphic activity since then (Copernican System) has been confined to the formation of a few large craters and the continuing minor modification of the lunar surface through the impact of comparatively small bolides.

19.3 Mars

The first close view of the Martian surface was provided by the Mariner 4 fly-by of 1964. Two more fly-by missions in 1969 by Mariners 6 and 7 provided further information, but detailed views of the planet's fascinating landforms had to await the arrival of the Mariner 9 orbiter towards the end of 1971. At first the surface was tantalizingly obscured by a huge dust storm, but after several months the atmosphere cleared to reveal some of the most spectacular landscapes in the Solar System.

During a period of a single year the Mariner 9 orbiter imaged almost the entire surface of Mars at resolutions of 1–10 km, with selected areas being imaged at higher resolutions of up to 100 m. This mission provided the basis for the initial mapping of the planet's surface and was complemented by two Soviet orbiters in 1971 and 1973. The Viking 1 and Viking 2 combined orbiter and lander missions in 1976 provided more extensive high resolution imagery totalling nearly 60 000 individual frames. In addition to monitoring changes on the surface during the slowly

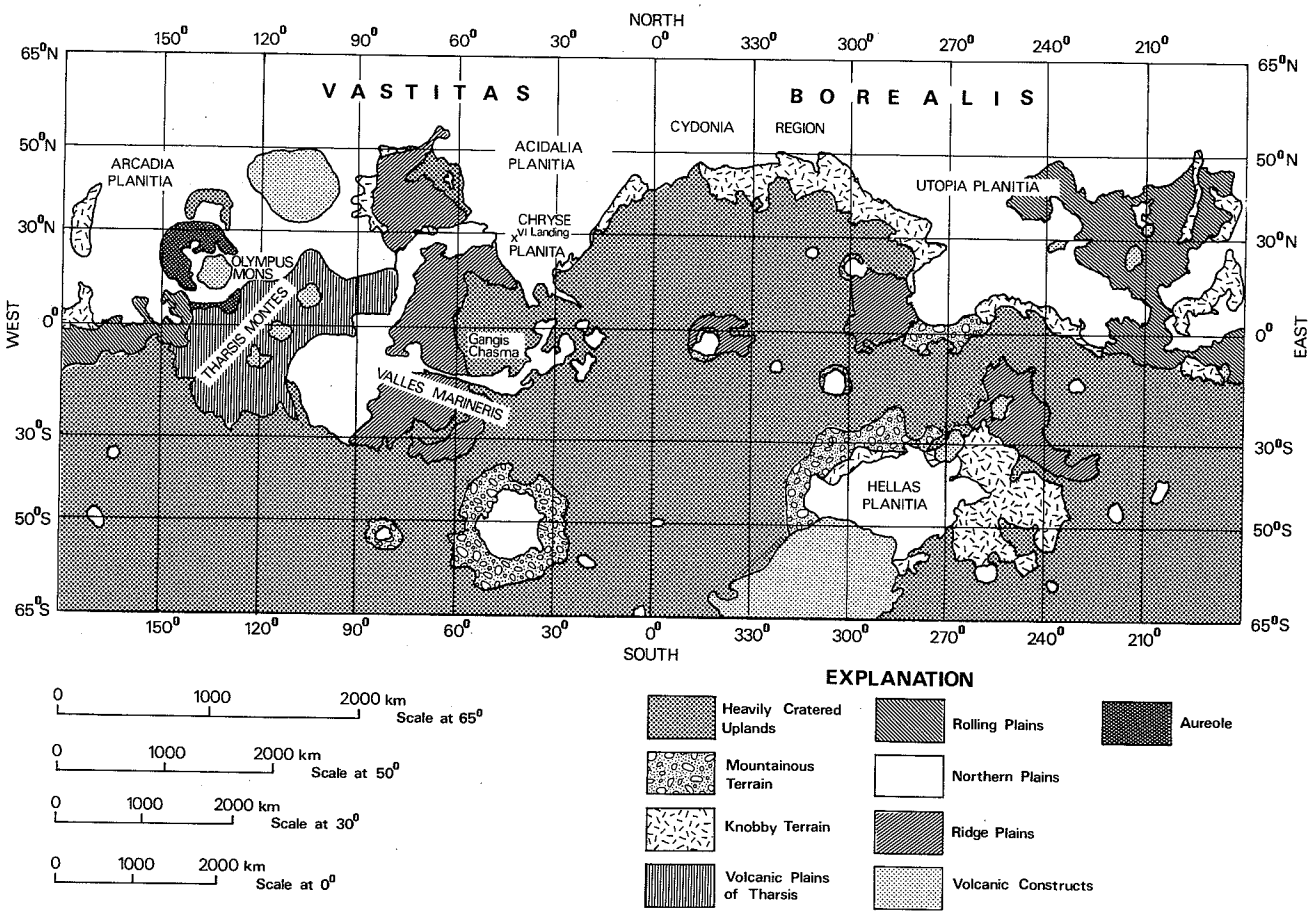

Fig. 19.5 *Geomorphic map of Mars between latitudes 65°N and 65°S constructed from Viking orbiter imagery. (Based on V. R. Baker, 1981,* Progress in Physical Geography *5, Fig. 1, p. 474, modified from the Geologic Map of Mars by D. H. Scott and M. H. Carr (1978)* United States Geological Survey, Miscellaneous Geologic Investigations, Map *I-1083.)*

changing Martian seasons the two Viking lander probes provided close-up views of landforms around the landing sites and the first analyses of the Martian regolith.

Maps constructed from Mariner and Viking orbiter imagery indicate a wide variety of terrain types on Mars and the operation of a range of geomorphic processes, including fluvial and aeolian erosion and deposition, weathering, mass movement and periglacial activity, as well as impact cratering. At the very broad scale the planet may be divided into two hemispheres separated by a great circle inclined at about 35° to the equator. The southern hemisphere is heavily cratered, whereas the northern hemisphere is on average lower and consists mostly of plains. The reason for this contrast is not known. At a more detailed scale nearly a dozen major morphological provinces have been identified (Fig. 19.5; Table 19.3).

19.3.1 Impact craters

Although impact craters are a very common element of most planetary landscapes, many of those on Mars have very special characteristics which make them unlike anything observed elsewhere in the Solar System (Fig. 19.6). The form of the ejecta, which occurs as overlapping lobes, implies some form of fluid flow; indeed, these features have been termed 'splosh' craters. The most probable explanation for this unusual morphology is that the material disturbed on impact included subsurface ice (permafrost) which, either as a gas or liquid, became incorporated into the ejecta to form a debris flow. Secondary craters are also found which indicate that ballistic processes do operate to some extent. An intriguing finding is that the distribution of the debris lobe type craters appears to be related to latitude and altitude; this may be indirect evidence of a variation in the depth of permafrost over the planet, with ordinary ballistic impact type craters only forming where the permafrost is confined to great depths.

Table 19.3 Principal morphological provinces of Mars

MORPHOLOGICAL PROVINCE	MORPHOLOGICAL CHARACTERISTICS
Heavily cratered uplands	Widespread hilly and cratered terrains of the equatorial and southern highlands
Mountainous terrain	Ejecta and uplifted blocks of ancient terrain caused by large impacts
Knobby terrain	Fretted uplands and isolated flat-topped residuals formed as erosional remnants along the boundary between the heavily cratered uplands and northern plains
Volcanic plains of Tharsis	Relatively young lava flows originating from the Tharsis Montes volcanic province
Rolling plains	Intermediate age lava flows originating from the Elysium volcanoes or other sources
Northern plains	Complex lowland exhibiting evidence of ice-contact volcanism, permafrost features and aeolian modification
Ridged plains	Relatively old lava plains that show prominent ridges
Volcanic constructs	Individual large volcanoes including Olympus Mons, Alba Patera and Elysium Mons
Aureole	Complex terrain of elongate hills and ridges occurring around the margins of certain volcanoes
Chaotic terrain	Blocky, fractured terrain apparently developed through the collapse and subsidence of the heavily cratered terrain
Valleys and channels	Includes the highly modified landscape of Valles Marineris and various valley and channel features attributed to fluid flow erosion

Source: Based on terrain types identified in Fig. 19.5 and described in V. R. Baker (1981) *Progress in Physical Geography*, **5**, pp. 474–6.

Fig. 19.6 *The 18 km diameter Martian crater Yuty located at latitude 22°N, longitude 34°. Several sheets of ejecta can be observed, each with well-developed lobes. These types of craters are common in a belt lying within 30–40° of the equator. Since the small crater adjacent to Yuty has experienced only partial burial the layers of ejecta must be relatively thin. (Viking 1 image, World Data Center A for Rockets and Satellites.)*

19.3.2 Volcanic and tectonic features

On the basis of our present knowledge Mars possesses the largest volcanoes in the Solar System. Olympus Mons reaches 26 km above the surrounding plain from which it is separated by a scarp up to 8 km in height. A number of collapse structures are found around the summit, and the caldera complex alone is some 80 km across (Fig. 19.7).

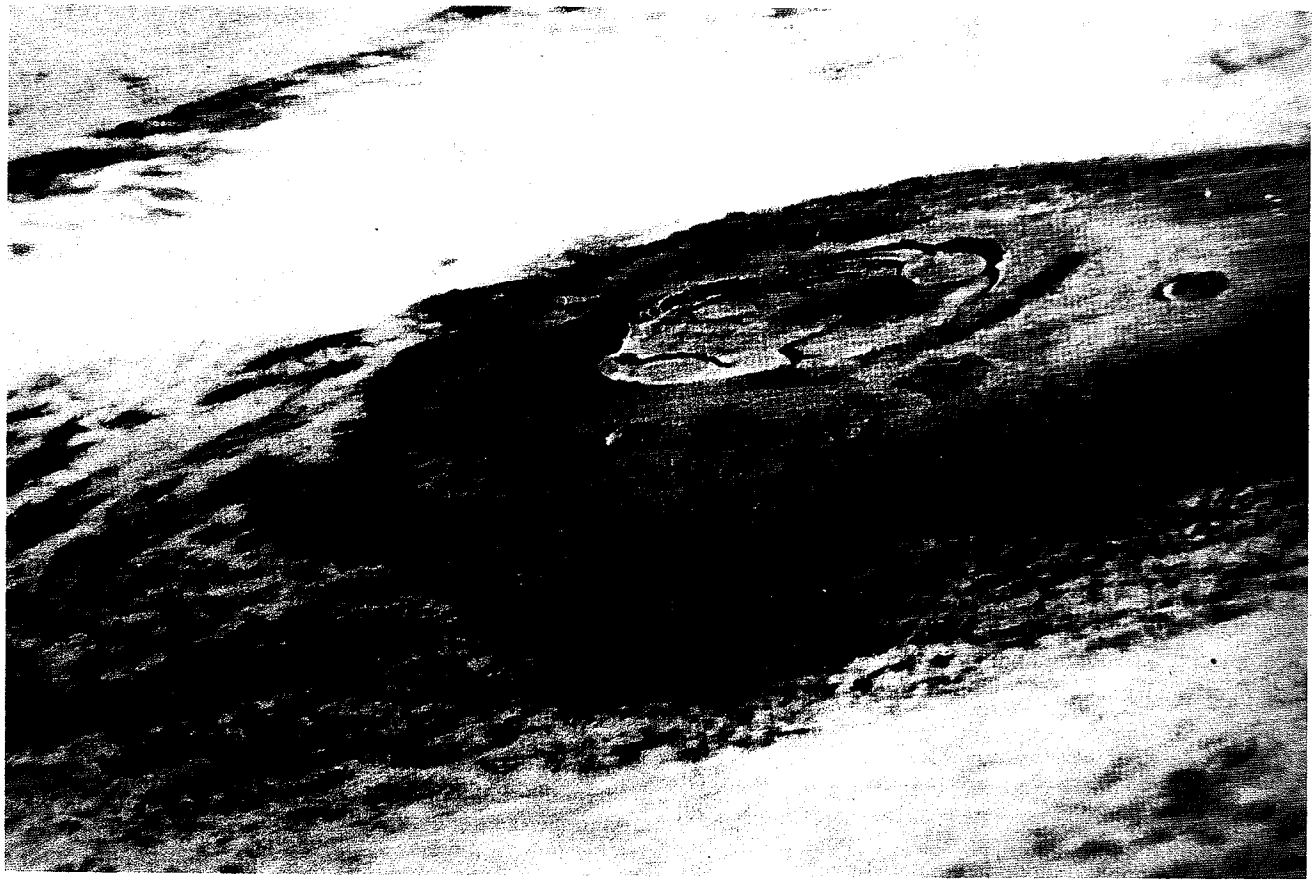

Fig. 19.7 *Oblique view of Olympus Mons, one of the largest volcanoes known in the Solar System. Based on the density of cratering it has been estimated that Olympus Mons is some 400 Ma old, although this may simply be the age of the youngest flows, the whole edifice probably having been built over billions of years. By comparison, volcanoes on Earth rarely survive more than a few million years before being destroyed by erosion. (Viking image, World Data Center A for Rockets and Satellites.)*

The morphology of Olympus Mons is broadly comparable to the shield volcanoes of Hawaii, but these two landforms differ dramatically in size with Hawaii (the largest shield volcano complex on Earth) rising only a mere 10 km from the ocean floor! (Fig. 19.8). The great height of some Martian volcanoes should not surprise us because the lower surface gravity on Mars (only 38 per cent of that of the Earth) means that large volcanic edifices there weigh less than their terrestrial counterparts and consequently do not load the underlying crust to the same extent.

The larger Martian volcanoes are all of the shield type and are associated with massive lava flows. Alba Petera is 1500 km across and dwarfs even Olympus Mons. It has a modest elevation of only 6 km so its flanks are inclined at a very shallow angle. It was thought initially to be an ancient degraded structure, but Viking imagery has revealed numerous juvenile features on its slopes including sheet flows and lobe fronts. These large shield volcanoes are concentrated in an area of probable 'mantle' upwelling known as the Tharsis Montes volcanic province (Fig. 19.5). This is a massive crustal bulge which formed about 3.9 Ga BP and its

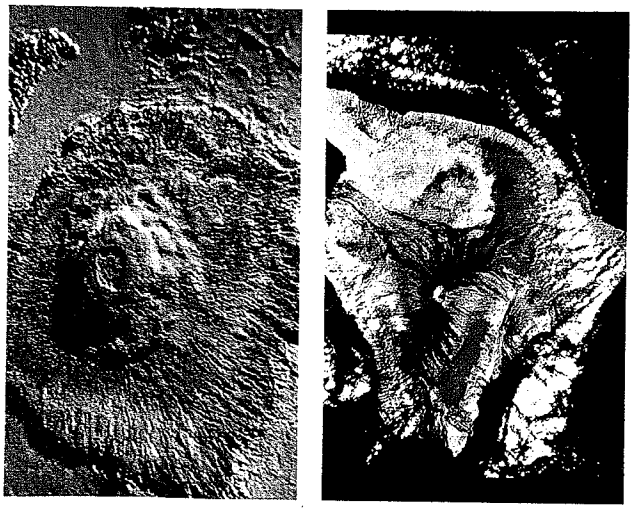

Fig. 19.8 *Olympus Mons (left) compared with the shield volcano of Hawaii (right). Olympus Mons is 650 km in diameter and is composed of thousands of individual lava flows. Its caldera complex alone is over half the size of the whole subaerial part of Hawaii shown here. (Olympus Mons – Viking 1 image, World Data Center A for Rockets and Satellites; Hawaii – Landsat mosaic courtesy N. M. Short.)*

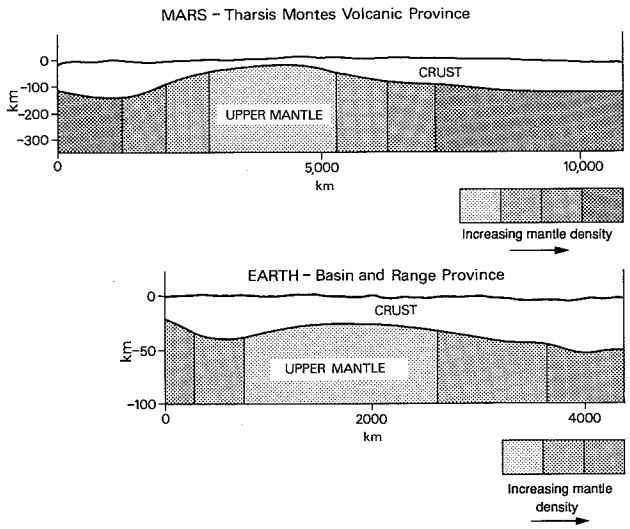

Fig. 19.9 *Combined crustal density (Pratt) and crustal thickness (Airy) isostatic model for the Tharsis Montes volcanic province of Mars in comparison with a similar model for the Basin and Range Province in the western USA. (Modified from N. H. Sleep and R. J. Phillips (1979)* Geophysical Research Letters ***6***, *Fig. 2, p. 805. Copyright by the American Geophysical Union.)*

origin may be similar to that of the Basin and Range Province of the western USA (Fig. 19.9).

In addition to extensive lava flows there is evidence in the form of blankets of tephra that many Martian volcanoes have experienced explosive episodes early in their history. This could be explained by the explosive consequences of magma penetrating a frozen, water-saturated regolith. Subsequently, the amount of near-surface water declined and later volcanism was confined to lava eruptions and the formation of dome and shield volcanoes.

A range of tectonic features have been identified on the Martian surface, many in association with volcanic structures. Far and away the most impressive of these is the system of canyons collectively called the Valles Marineris. This complex graben-like feature is some 5000 km long, averages around 200 km wide and is up to 7 km in depth. Some idea of the size of this landform can be gained by imagining a canyon four times as deep and about fifteen times as broad as the Grand Canyon, stretching coast to coast across the USA. The Valles Marineris has clearly formed through the effects of large-scale tensional stress in the Martian crust and its possible association with the Tharsis bulge suggests that it may be of a similar age.

19.3.3 Weathering

Although contrasting starkly with the Earth, the atmosphere and surface conditions on Mars are closer to our own planet than any of the other bodies of the Solar System. In spite of marked differences in atmospheric pressure, atmospheric composition and surface temperatures (Table 19.1) there are some apparent similarities in weathering processes. Analyses carried out by the Viking landers, although failing to confirm the presence of life, provided valuable data on the physical and chemical properties of surface materials. Some of the boulders observed in Viking lander imagery (Fig. 19.10) may have been formed by *in situ* weathering, but it

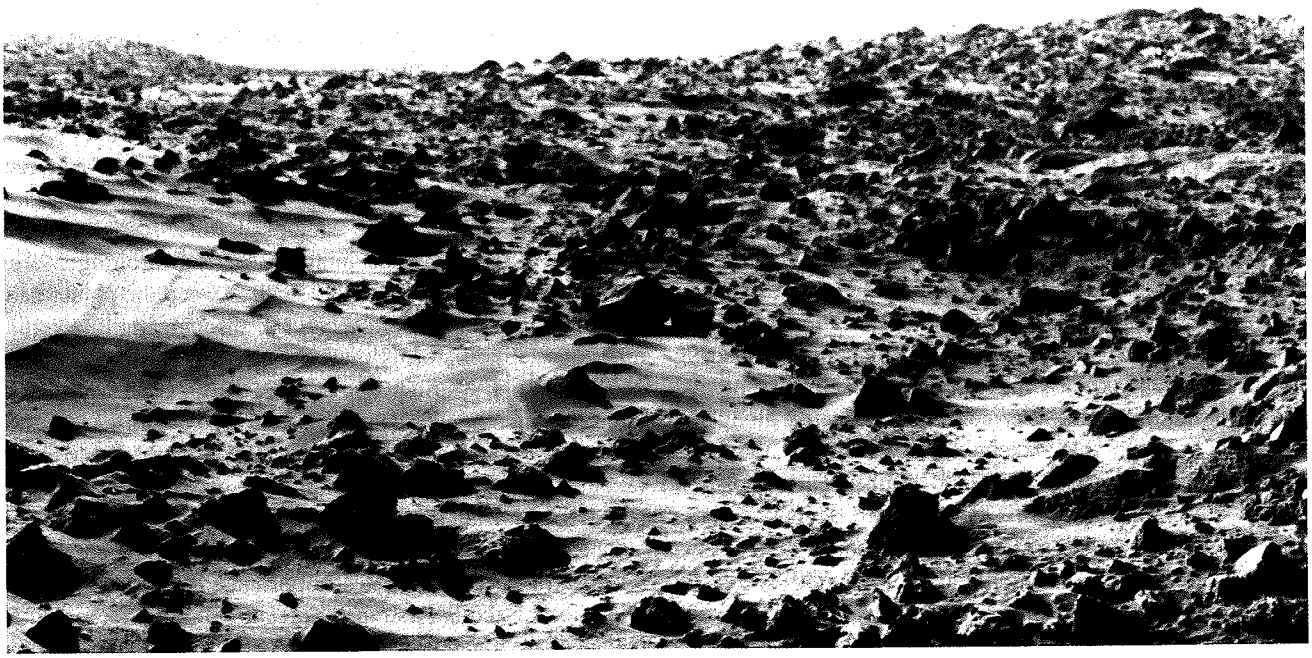

Fig. 19.10 *Ground view across Chryse Planita from the Viking 1 landing site on Mars. Large numbers of boulders, up to 1 m or so across, can be seen in addition to drifts of fine-grained material. (Viking 1 mosaic, World Data Center A for Rockets and Satellites.)*

is more likely that they are simply ejecta from impact events.

A possible explanation for the formation of the fine-grained material which mantles much of the surface at both the Viking landing sites is salt weathering since the Martian soil appears to be rich in sulphur, probably in the form of sulphate salts. The presence of a thin salt crust (sometimes misleadingly described as 'duricrust' by planetary geologists) is also indicated from the observation that surface material broke into small cohesive fragments where it was disturbed by the sampling arm attached to the Viking landers. Frost weathering may also be significant on Mars since both water and carbon dioxide ice have been identified on the surface, but as with other Martian geomorphic processes there is far more speculation than conclusive data. The closest terrestrial analogues are the cold, arid valleys of Antarctica. There is certainly a seasonal cycle of frost deposition on Mars and a thin, bright surface covering was seen to form during winter at the Viking 2 lander site.

19.3.4 Slopes and mass movement

The abundance of high escarpments on Mars provides considerable scope for the operation of mass movement mechanisms; certainly the scale of such processes exceeds anything occurring on Earth. In the Valles Marineris concave chutes separate the comparatively flat upland surface from the canyon itself (Fig. 19.11). These chutes lead down either into talus slopes or into a 'spur-and-gully topography' made up of alternating ridges and swales. The talus slopes typically have a mean angle of around 30° and in some cases have a vertical drop of several kilometres. In a study employing Viking imagery, 25 large landslides ranging in size from 40 to 7500 km^2 were identified in the Valles Marineris; one of these was seen to be recessed up to 30 km into the escarpment wall.

One explanation for these massive landslide features involves dry avalanching of unconsolidated material. This implies that, at least in some areas, the surface is covered by a thick, non-cohesive regolith possibly resulting from the shattering of bedrock through bolide impacts. Another, now more favoured, hypothesis is that the undermining of free faces by sapping, involving the evaporation of ground water or permafrost ice, is the primary landslide-triggering mechanism. This process may also have been instrumental in the formation of the **fretted terrain** located along the boundary between the ancient heavily cratered highlands and the sparsely cratered lowland plains. This transition zone consists of vast debris aprons with a characteristic convex lobate form and appears to represent an area of outward flow of debris from highlands to lowlands. The fairly uniform height of the eroding escarpments within the fretted terrain at between 1 and 2 km has been interpreted as indicating that scarp retreat may be controlled by the depth to which ice-rich permafrost extends.

Fig. 19.11 *Large landslides on the south wall of Gangis Chasma in the Valles Marineris region of Mars. The escarpment running left to right across the centre of the image is about 2 km high and separates a plateau region (top) from the floor of Gangis Chasma (bottom). Some of the landslides show backward rotation (arrowed), a feature characterizing rotational slumps on Earth. The area shown is about 60 km across. (Viking 1 mosaic, World Data Center A for Rockets and Satellites.)*

19.3.5 Aeolian processes and landforms

With a lack of surface water, the absence of any vegetation to stabilize the surface, and the presence of high winds and fine sediment it is not surprising that aeolian landforms are abundant on Mars (Fig. 19.12). There is a vast erg surrounding the north polar region, wind-laid dust and ice deposits at the poles themselves and numerous depositional and erosional forms in the equatorial zone. Although now recorded in detail by the imaging systems orbiting Mars, the great dust storms that periodically sweep the planet had long been observed from the Earth through high-powered telescopes. Such storms may shroud the whole planet, as occurred when Mariner 9 arrived in 1971, and can last for up to four months. Wind speeds can exceed 140 m s^{-1} (around 500 km h^{-1}) compared with a typical maximum of 30–40 m s^{-1} (about 120–160 km h^{-1}) on Earth; dust may rise up to 70 km above the Martian surface.

The much lower atmospheric pressure on Mars compared with Earth (Table 19.1) has important implications for the operation of aeolian activity. Threshold drag velocities, for instance, are much larger on Mars (Fig. 19.13); consequently saltating grains have about twenty times the velocity of similar-sized particles on Earth and the potential for aeolian

Fig. 19.12 *Dunes in the ancient cratered terrain of Mars located at latitude 47°S, longitude 340°. Most of the dunes are of the transverse ridge and barchanoid ridge type, but isolated barchans are also visible (arrowed). The area shown is about 60 km across. (Viking 2 image, World Data Center A for Rockets and Satellites.)*

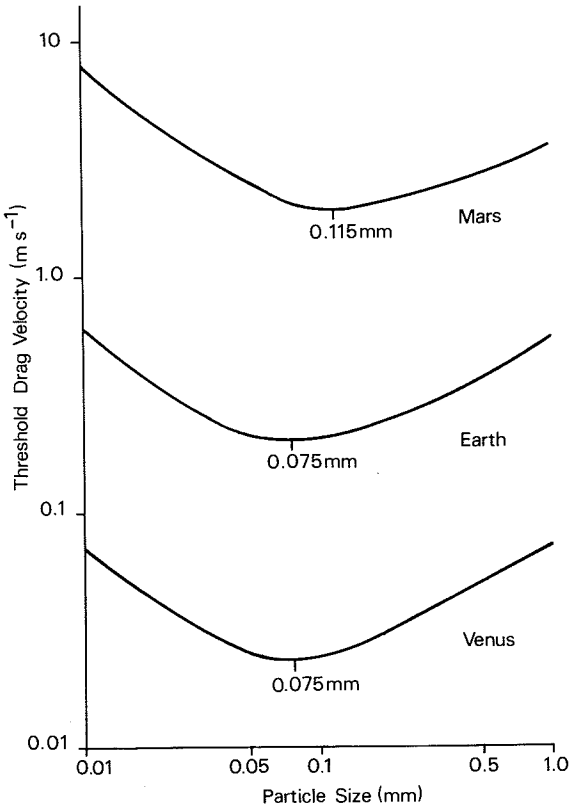

Fig. 19.13 *Threshold drag velocity in air as a function of particle size on the Earth, Mars and Venus. Note that for 0.2 mm sized particles this velocity may be ten times greater on Mars than on Earth. Saltating grains on Mars have about ten times the momentum and one hundred times the kinetic energy of those on Earth. The reasons for the higher threshold drag velocity for particle sizes less than about 0.1 mm are not known for certain but are probably associated with interparticle cohesion and aerodynamic effects. (Modified from R. Greeley (1985)* Planetary Landscapes, *Allen and Unwin, London, Fig. 3.36, p. 66.)*

erosion is therefore considerable. Silt to clay-sized particles seem to predominate on the Martian surface, but sand-sized aggregates can apparently form through the electrostatic bonding of this finer material. The dunes observed on Mars are probably formed largely from these aggregates and are therefore in some respects analogous to clay dunes on Earth. Wind-tunnel experiments suggest, however, that such sand-sized aggregates may have a short life span since at slightly above Martian threshold drag velocities they rapidly break up into fine fragments around 20 μm in diameter. The image of the destruction of these aggregates as they smash into rock surfaces at high velocities has given rise to the vividly descriptive term **kamikaze grain**.

Inspection of Mariner and Viking orbiter imagery has revealed a wide variety of both erosional and depositional aeolian forms on Mars. Morphologically, many of these are very similar to landforms recorded from terrestrial deserts, but the great size of some features exceeds any analogous forms occurring on Earth. Various dune patterns have been identified; those of the Hellespontus area, for instance, have a crescentic ridge form reminiscent of terrestrial dunes in central Asia. Massive barchanoid and transverse forms have also been recorded as well as the coalescence of individual barchans, a feature well known from terrestrial deserts (Fig. 19.14).

Aeolian erosional landforms include modified crater rims, linear grooves, streamlined ridges and fluted cliffs. An aeolian origin is implied where parallel series of linear ridges and grooves extend over large distances, some of the forms seen on Mars being morphologically comparable to terrestrial yardangs. The distribution of aeolian erosional landforms is localized and this suggests that they may only form where there are friable surface materials. Estimates of rates of aeolian erosion on Mars range from a negligible 0.001 mm ka^{-1} for the lowland plains to a maximum of around 0.1 mm ka^{-1} in parts of the heavily cratered highlands. Although the apparent lower density of craters at high latitudes may be due in part to the blanketing effect of aeolian deposits, and thus imply the active deflation of material from elsewhere, measurements from the Viking landers have demonstrated that current rates of aeolian erosion and deposition are extremely low.

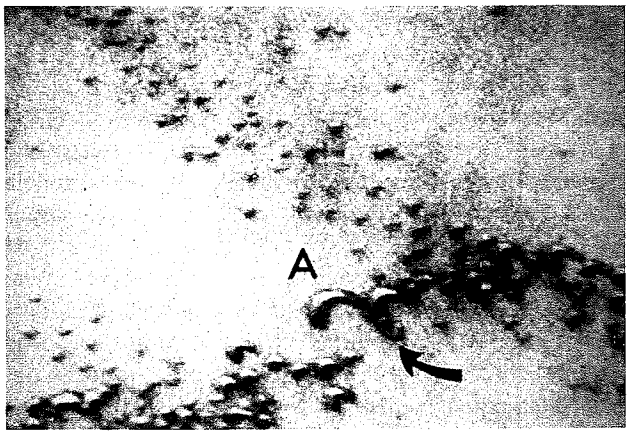

Fig. 19.14 The arm of a migrating barchan (A) on Mars coalescing with another barchan downwind (arrowed) The labelled barchan is about 500 m across and 200 m long and is situated near the southern edge of the erg located at latitude 73°N, longitude 39°50′. All the dunes visible are migrating towards the bottom of the image, that is, in an approximately easterly direction. (Viking 2 image, World Data Center A for Rockets and Satellites.)

19.3.6 Periglacial processes and landforms

It could be argued that 'periglacial' is an inappropriate term to apply to geomorphic processes on Mars since there is no firm evidence that glaciers have ever existed on the planet. None the less, in its broader sense, as applied in Chapter 12, the term is appropriate as it refers to environments characterized by low temperatures with fluctuations above and below freezing. Although water in its liquid state is known not to exist in significant quantities on the present-day Martian surface, locally it may occur at shallow depths in the regolith in the equatorial zone. But freeze–thaw activity and associated frost creep may have been widespread in the past when mean temperatures were probably rather higher and surface water may have been more abundant. If salt is an important constituent of the present-day surface, freeze–thaw may be currently active since liquid saline solutions might be able to exist during the day at low latitudes.

The possible extent of periglacial activity on Mars is suggested by the presence of patterned ground recorded in high resolution Viking imagery. Although the polygonal patterns observed are certainly similar to terrestrial patterned ground, some occur at a much larger scale than analogous forms on Earth. Ice-wedge polygons on Earth are typically 1–100 m across, but some of the Martian polygons are 5–10 km in diameter, the cracks themselves being hundreds of metres across. If they are indeed periglacial phenomena it is likely that they have been generated by temperature changes of considerable duration extending to great depths within the Martian permafrost, rather than by the seasonal temperature fluctuations largely responsible for ice-wedge polygon formation on the Earth. Alternative explanations for these phenomena exist, however, including the contraction of cooling lava and extension associated with tectonic mechanisms.

The present water content of the Martian permafrost is not known but there is abundant morphological evidence for a high ice content in the past. Likely thermokarst features include alases (irregular depressions) and thermocirque topography (embayed escarpments; see Section 12.3.2.4). Such landforms, arising from the melting of ground ice, are best developed in terrestrial periglacial environments where the ice content is high. The **chaotic terrain** occurring in parts of the Martian equatorial zone has been widely interpreted as the result of large-scale ground collapse but the size of these features on Mars is much greater than terrestrial thermokarst forms (Fig. 19.15).

There is a clear latitudinal control over the operation of permafrost-related processes on Mars. Estimates of the likely heat flow from the planet's interior indicate that the maximum permafrost depth ranges from about 1 km at the equator to around 3 km at the poles. Under the present climatic regime permanent ice can probably exist to within a few centimetres of the Martian surface at latitudes above about 40°. Local melting of ice-rich permafrost to produce thermokarst and related landforms could result from a variety of mechanisms including volcanism and bolide impacts. More widespread melting might be precipitated by climatic changes, while scarp retreat could lead to the release of liquid water confined at depth within the permafrost layer.

19.3.7 Polar terrains

The frost caps of Mars expand to cover up to 30 per cent of the planet's surface area during the Martian winter but retreat to small residual 'ice caps' covering only 1 per cent of its area in the summer. The remnant north polar ice cap is largely composed of water ice, but the nature of the permanent southern cap is less certain and it may consist of both frozen water and carbon dioxide. The seasonal frost blanket is predominantly formed by the freezing of atmospheric carbon dioxide, although it probably also includes dust particles coated by water ice.

The perennial ice caps contain layered deposits which have been partially exposed by the formation of deep canyons. This is the **layered terrain** in which alternating bright and dark bands up to 30 m thick have been observed exposed along canyon walls. This banding may represent changes in the ratio of dust to ice deposited on the ice caps, and it has been suggested that such fluctuations ultimately have a climatic origin. Indeed, it has been speculated that Mars may have experienced cycles of climatic change similar to those on Earth during the Late Cenozoic Ice Age and that there may even be a common cause in the Milankovitch

Fig. 19.15 *The head of a Martian outflow channel containing an extensive area of chaotic terrain (right centre of image). Detailed examination of this region has revealed slumped and collapsed blocks up to 10 km long lying at the base of steep escarpments rimmed by arcuate features. Vast quantities of debris have clearly been removed and this may have been accomplished by the catastrophic release of water from the melting of ice-rich permafrost. The area shown is about 300 km across. (Viking 1 mosaic, World Data Center A for Rockets and Satellites.)*

mechanism (see Section 14.3.2). The lack of fresh impact craters in the layered terrain certainly indicates that in Martian terms the surface features in this region are relatively young and that the layered deposits must be accumulating rapidly compared with the recent cratering rate.

As already mentioned, there is no unequivocal evidence for glacial erosion on Mars and it certainly seems that the existence of flowing ice is ruled out in the present Martian environment. Nevertheless, glacial processes have been proposed as an explanation for the so-called outflow channels on Mars (see Section 19.3.8) because their forms are, in some respects, similar to terrestrial glacially eroded valleys. An argument in favour of the glacial theory is the comparable scale of the Martian and terrestrial forms, but a glacial origin for outflow channels is difficult to reconcile with their concentration within 30° of the Martian equator. As we shall now see, there is no shortage of alternative hypotheses to explain these and other channel forms on Mars.

19.3.8 Channels

No landforms on the Martian surface have generated more controversy than the range of channel features first seen on Mariner 9 imagery and subsequently investigated in detail using the higher-resolution Viking orbiter data. In nearly all cases these forms are most accurately described as valleys, but as the term 'channel' has gained wide currency among planetary geomorphologists we will retain it here. Three main types of channel have been recognized.

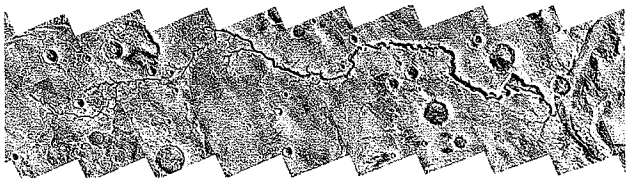

Fig. 19.16 *Nirgal Vallis, an 800 km long runoff channel on Mars located at latitude 28°S, longitude 40° and incised into old cratered terrain. See Figure 1.2 for detail from part of the channel network towards the left-hand edge of the area shown here. (Viking 1 mosaic, World Data Center A for Rockets and Satellites.)*

Fretted channels have wide, smooth floors and steep walls and are found in the fretted terrain marking the transition between the heavily cratered uplands and the lightly cratered lowland plains. The presence of large debris flows where these channels extend into the lowlands indicates that they have formed through escarpment retreat by mass movement.

Runoff channels, which are connected to form dendritic networks, are in many ways similar to terrestrial fluvial systems; they are found throughout the older cratered terrain (Fig. 19.16). When first observed they were simply attributed to surface runoff processes and were thus considered to be ancient features related to a past pluvial epoch on Mars. The junction angles of these networks are, however, much less acute than in most terrestrial fluvial systems. By analogy with morphologically similar forms which occur in certain environments on the Earth, such as on the Colorado Plateau in the south-west USA (Fig. 1.3), headward erosion by spring sapping is now thought to be a more likely mode of formation (Fig. 1.2). Meltwater from ice-rich permafrost is the likely source of the required water.

Outflow channels are much larger features tens of kilometres wide and hundreds of kilometres long (Fig. 19.15). They generally lack tributaries and most originate within chaotic terrain or large concave depressions. Of particular interest is the variety of bedforms seen on the floors of outflow channels including scour marks, longitudinal grooves and streamlined upland remnants (Fig. 19.17). Scour marks and other erosional and depositional forms extend into the plains on to which the mouths of outflow channels open. Although they are widely regarded as having been formed

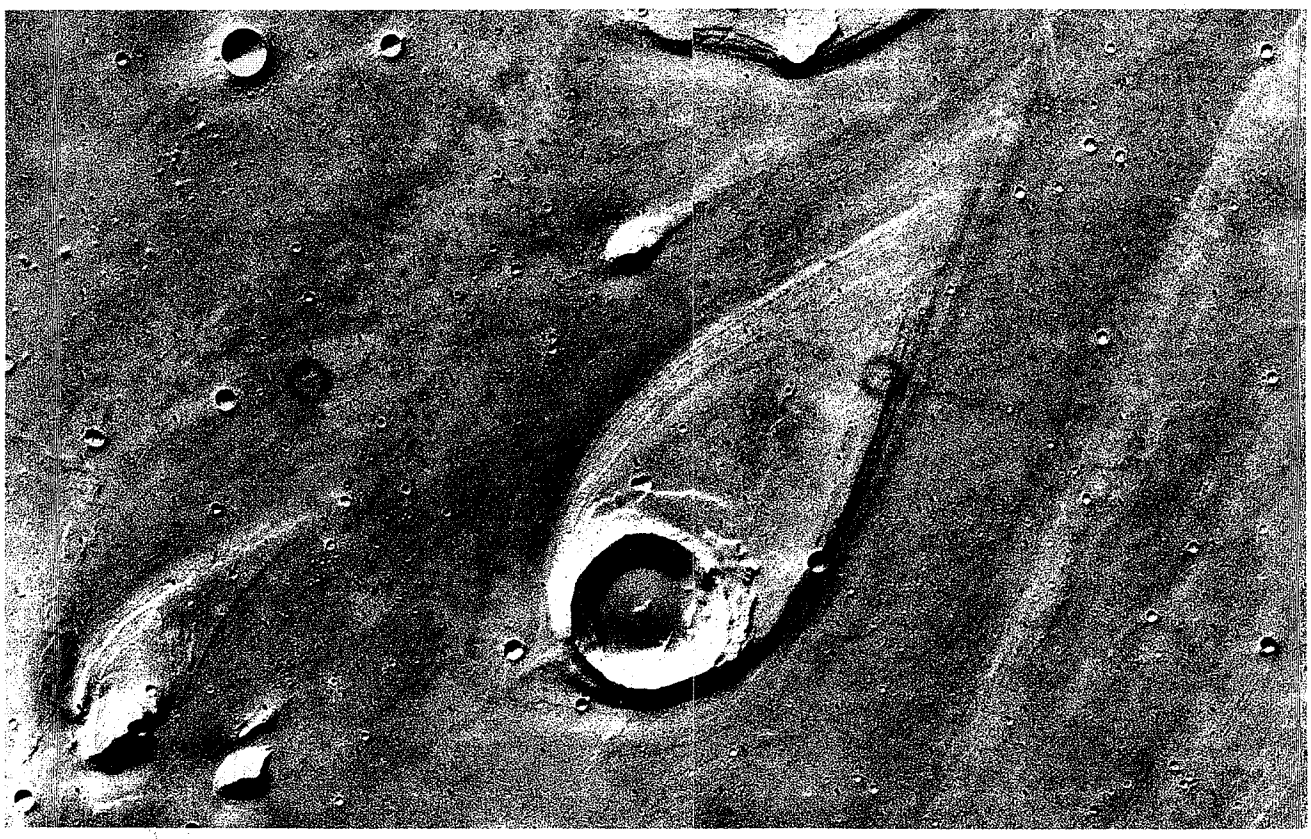

Fig. 19.17 *A streamlined 'island' about 40 km in length representing an eroded remnant of a former plateau located at the mouth of Ares Vallis, an outflow channel on Mars located at latitude 20°N, longitude 31°. The flow from the lower left to the upper right diverged around the crater rim forming a tapering tail downstream. (Viking 1 mosaic, World Data Center A for Rockets and Satellites.)*

by some kind of fluid flow there is little agreement as to the particular fluid agent involved. The erosive agents proposed include water, ice, wind, debris flows, liquefied crustal material and low-viscosity lava.

Detailed comparisons between the form of outflow channels and the morphology of the Channeled Scabland of eastern Washington and Oregon in the USA (see Section 11.4.1) have led to the suggestion that the Martian channels similarly owe their form to the action of catastrophic floods. Although the outflow channels are generally much larger than their terrestrial equivalents, this may be explained by the significantly different conditions of surface gravity and atmospheric pressure on Mars. The lower surface gravity, for instance, could allow the transportation of cobble-sized material in suspension, and it is likely that catastrophic floods could attain a sediment concentration of up to 60–70 per cent by volume. Formation of the outflow channels could, therefore, have been accomplished very quickly, perhaps in a matter of a few days or weeks. Even accepting the dominant role of some kind of water flow in sculpturing their overall form, outflow channels have clearly also been extensively modified by a range of other processes, including thermokarst development, impact cratering, aeolian erosion, spring sapping and a variety of mass movement processes.

If outflow channels are accepted as essentially water-eroded landforms, a crucial problem remains the source of such water which clearly must have been present in very large quantities. An initial proposal was that volcanic eruptions below glaciers led to rapid melting and the catastrophic release of water, but this hypothesis requires the existence of significant ice sheets outside the polar regions. A related idea is the melting of ice-rich permafrost associated with volcanic activity, although this would be a far less efficient process for rapidly generating large quantities of meltwater.

Another hypothesis involves the catastrophic release of artesian water under high pressure. This possibility arises from the postulated existence of an aquifer system extending from about 1 km to 5 or 10 km below the Martian surface and confined by a thick, impermeable, overlying permafrost layer. This mechanism has the advantage of simultaneously accounting for catastrophic water release and the formation of chaotic terrain at the head of outflow channels through the collapse of the surface on the removal of the underlying water.

19.3.9 History of landscape development

In the absence of dated surface materials from samples returned to Earth, the chronology of landscape development on Mars rests on estimates of cratering rates. A range of time scales have been proposed; one of these gives the age of the oldest crust as 4.2–4.3 Ga, volcanic activity in the Tharsis region at between 3 and 1 Ga BP, and the major phase

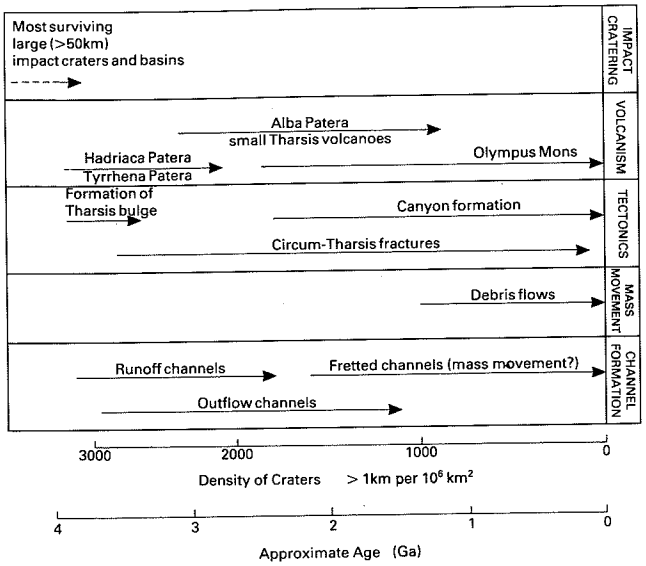

Fig. 19.18 *A possible chronology for the Martian landscape. (Modified from M. H. Carr (1981)* The Surface of Mars. *Yale University Press, New Haven, Fig. 16.1, p. 202.)*

of channel formation from 4 to 3.7 Ga. Another chronology suggests more recent activity with highland lava emplacement between 3.9 and 0.3 Ga BP and Tharsis region volcanism starting about 0.5 Ga BP. More detailed investigations of cratering rates in the outflow channels suggest that they formed from 0.5 to 2 Ga BP, while the runoff channels are considered to be rather older. The most modern features of the Martian landscape are some of the dune formations which, as repeated Viking orbiter observations show, are currently active. Figure 19.18 gives a very tentative chronology for the main landforming episodes on Mars which will no doubt be considerably revised when rock samples eventually become available for radiometric dating.

19.4 Mercury

Before the fly-by Mariner 10 mission in 1974 Mercury was the least known of the inner planets. Because of its comparatively small size and proximity to the Sun no surface details could be discerned from the Earth. The Mariner 10 fly-by provided adequate coverage of nearly half of the planet at resolutions from 4 km to 100 m. First impressions are that the surface is very like that of the Moon (Fig. 19.19). Impact craters are the predominant landform and most of the features associated with lunar craters are also found on Mercury. Minor differences can be attributed largely to the higher surface gravity of Mercury; ballistic ejecta, for instance, are found closer to the primary impact crater.

A major contrast with the morphology of the Moon, however, is provided by the occurrence of lobate scarps. These appear to be associated with thrust faults resulting from crustal compression of global extent. It has been sug-

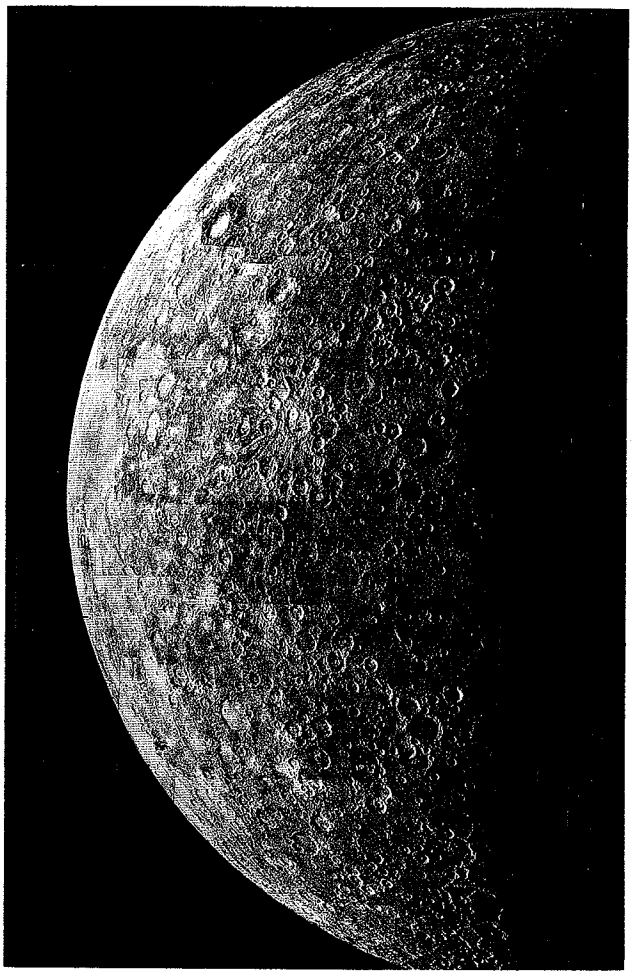

Fig. 19.19 *The surface of Mercury as seen on approach during the Mariner 10 fly-by mission. (Mosaic from the* Atlas of Mercury, *Fig. 18, World Data Center A for Rockets and Satellites.)*

gested that an episode of global contraction may have resulted from the cooling and shrinking of Mercury's large core and the stresses imparted by the slowing of the planet's rate of rotation due to its gravitational interaction with the Sun.

Impact features on Mercury range in size from the smallest craters resolvable in Mariner 10 imagery up to the Caloris Basin, a complex feature more than 1300 km across encircled by mountains up to 2 km high. Antipodal to the Caloris Basin is an anomalous region of hilly and lineated terrain which appears to disrupt earlier landforms. The creation of this **weird terrain**, as it has been termed, may have occurred as a consequence of the focusing of seismic waves generated by the massive impact event which formed the Caloris Basin itself.

The smooth plains of Mercury, which cover about 15 per cent of its surface, are similar in appearance to the lunar maria. Although no unequivocal volcanic features have been identified on Mariner 10 imagery, indirect evidence suggests that, like their lunar counterparts, these plains are at least primarily of volcanic origin. There are, for instance, many examples of material from the smooth plains filling craters clearly formed at an earlier stage.

In the absence of the kind of radiometrically based landscape chronology established for the Moon, any dating scheme for Mercury must rest on the assumption that it has experienced a lunar-type history of bombardment. Although there are similarities between the size frequencies and areal densities of impact craters on Mercury and the Moon, it has been questioned whether this necessarily indicates a temporal equivalence in bombardment history. It is perhaps safer, therefore, to talk in terms of a relative rather than an absolute landscape chronology for Mercury (Fig. 19.20).

19.5 Venus

Similarities in size, density and distance from the Sun make Venus in these respects the closest equivalent of Earth in the Solar System. There is a stark contrast, however, in the atmospheric properties of the two planets. Venus is blanketed by a thick atmosphere with a surface pressure some 90 times that of the Earth, while surface temperatures are around 480 °C. The dense atmosphere has prevented direct visual observation of the planet's surface from the Earth or by conventional orbiting satellite imaging systems. Instead our limited knowledge of the surface has so far come from the Soviet Venera landers and both Earth-based and orbiting satellite-based radar altimeters which are able to penetrate the atmosphere and provide data on variations in elevation over the planet.

The presently available radar data are of a resolution sufficient to pick out major morphological features, but inadequate to provide the detailed altitudinal information needed to determine unequivocally whether Venus has an

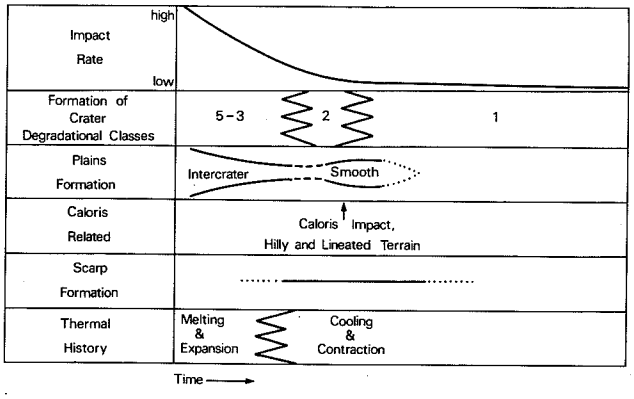

Fig. 19.20 *A relative chronology for the development of the surface features of Mercury. Note that other interpretations are possible. (After R. G. Strom (1979)* Space Science Reviews ***24***, *Fig. 38, p. 65.)*

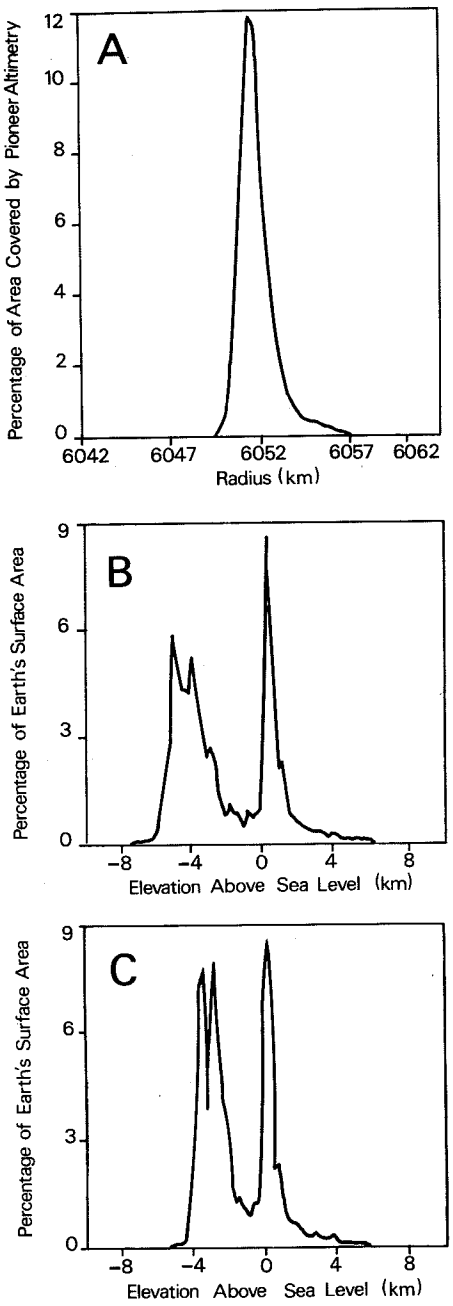

Fig. 19.21 *Hypsometric curves for Venus (A) and the Earth (B and C). Curve (B) represents the Earth's actual topography, whereas curve (C) represents the hypsometry with the loading effect of the oceans on the crust removed, the latter curve being the more appropriate for comparisons with Venus. (After J. W. Head* et al. *(1981)* American Scientist ***69****, Fig. 3, p. 617.)*

Earth-like topography dominated by the effects of plate tectonics, a Mars-like surface characterized by impact craters and volcanic landforms or a combination of the two. Nevertheless, one major morphological distinction is clear; the hypsometric curve for Venus displays a single peak in contrast to the Earth's bimodal distribution (Fig. 19.21). The latter has arisen largely from a combination of density contrasts between continental and oceanic crust, and the effects of plate tectonic mechanisms in continually generating new dense oceanic crust and sweeping lighter material on to the continental margins. We can surmise, therefore, that if plate tectonics does occur on Venus then it must be of a rather different form from that active on the Earth.

Examination of the gross topography of Venus does in fact suggest a number of features with at least a superficial resemblance to tectonic structures on the Earth (Fig. 19.22). For instance, a plateau feature known as Beta Regio appears to be a large domal uplift traversed by a rift with associated volcanoes, and indeed it has been likened to the East African Rift System. There are also extensive arcuate and linear troughs concentrated in the upland massifs, but these seem to be more analogous to Martian canyons. The extensive elevated area named Terra Ishtar reaches up to 11 km above the median elevation of Venus, and around this massif are a number of depressions which appear to be of volcanic origin. Another significant feature is a huge cone about 600 km across with an apparent summit caldera and this has been compared with the Martian shield volcano Olympus Mons. Numerous crater-like forms have also been recorded in the lowland areas; some of these may be volcanic, others impact craters, but most are of uncertain origin.

Further information bearing on the possibility of plate tectonics on Venus has been provided by the Soviet Venera 13 and Venera 14 landers. Chemical analyses of surface materials by these probes indicate the existence of tholeiitic basalts at the Venera 14 landing site, rocks typical of mid-oceanic spreading ridges on the Earth, and the presence of high-alkali basalts characteristic of terrestrial continental hot-spot volcanism at the Venera 13 site some 1000 km away. Although the presently available topographic data do not provide unequivocal evidence of the existence of plate tectonic structures on Venus, estimates of the likely rate of heat flow to the Venusian surface imply that a very large number of volcanic hot-spot centres must be present if spreading ridge systems are not available to dissipate heat.

Images of the surface returned by the Venera probes show a variety of terrains. The Venera 14 site is unusual in lacking unconsolidated material, but the other sites display fine to coarse debris resting on bedrock. Evidence of erosion of rock surfaces and the presence of angular rock fragments in Venera lander images indicate that the Venusian surface continues to experience geomorphic activity. Data on the extraordinary atmosphere provided by the Venera probes certainly suggest that chemical weathering should be extremely active. Since the partial pressure of H_2O increases with elevation the most vigorous weathering probably occurs in the upland regions.

In the absence of liquid water on the surface, at least in recent geological time, wind is presumably the main denudational agent. Theoretical calculations, in conjunction with

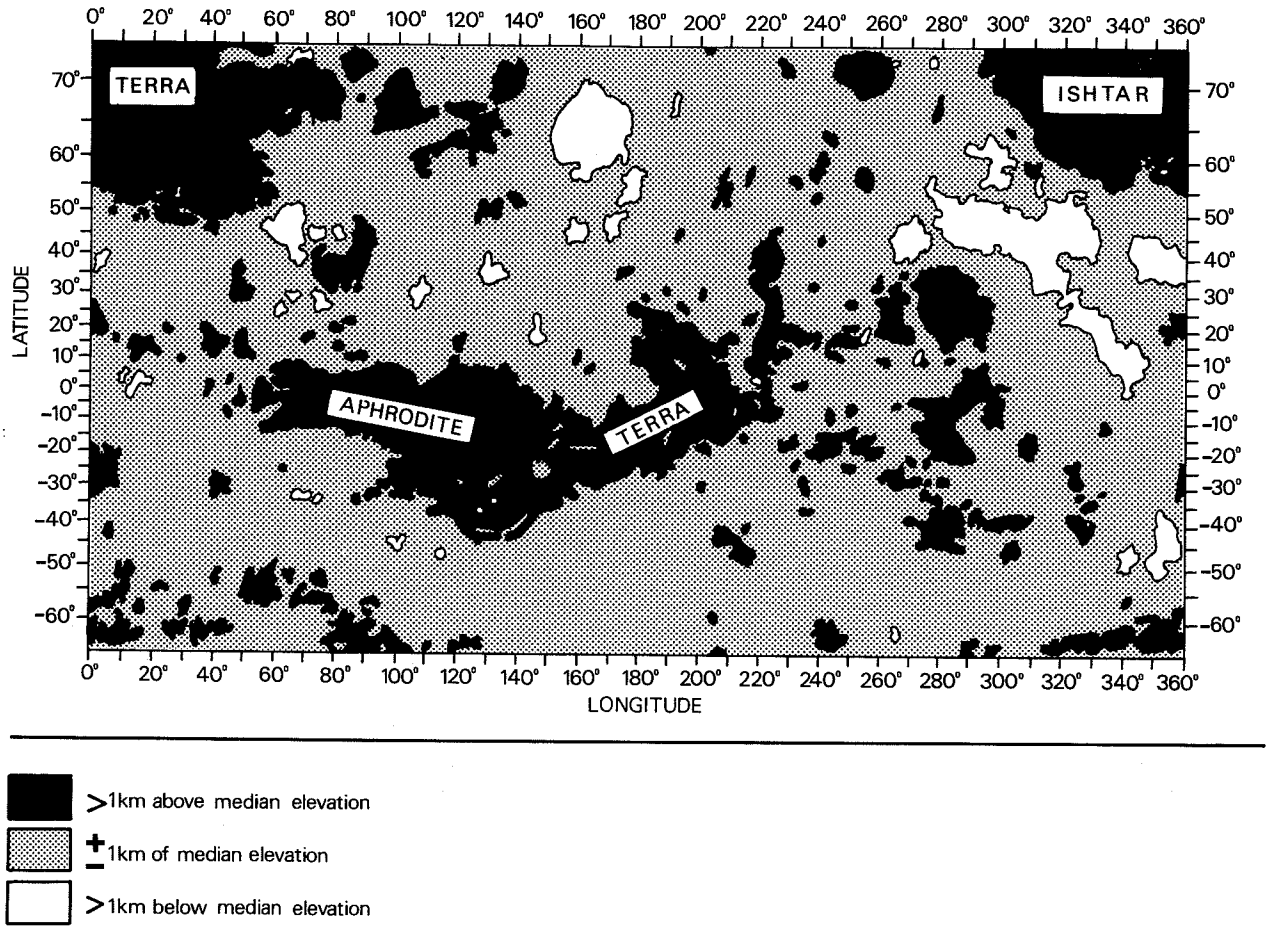

Fig. 19.22 Major topographic features of Venus based on radar altimetry. Note that the Mercator projection used greatly exaggerates the area covered by features at high latitudes. (After G. E. McGill (1982) Nature, ***296***, *Fig. 2, p. 14.)*

satellite data, indicate low wind speeds on the surface of Venus of around 1 m s^{-1}, but because the atmosphere is so dense particles up to 10 mm across can probably be transported (Fig. 19.13). Earlier in its history Venus may have been capable of retaining liquid water on its surface and so ancient fluvial features may yet be found. Of crucial importance to an understanding of the evolution of the Venusian surface is whether large impact basins remain from the Late Heavy Bombardment. This would indicate the extent to which endogenic and exogenic processes have subsequently modified the surface, but answers to these and other intriguing questions about the smaller-scale morphological features of the planet will have to await the return of high resolution radar imaging data from the Magellan probe launched from the space shuttle Atlantis in May 1989.

19.6 The moons of the outer planets

Beyond the inner Solar System lie the giant planets Jupiter, Saturn, Uranus and Neptune. Although these bodies lack a solid surface, they all possess orbiting satellites, some of which are of planet-sized dimensions. Until the Voyager programme of planetary exploration which began in the late 1970s little was known of the surface features of the rocky and icy satellites of the outer planets, and the first close-up images of the moons of Neptune were only received from Voyager 2 in 1989. The images that have so far been returned from the hugely successful Voyager probes have revealed landscapes with extraordinary characteristics, and which, in many cases, have no terrestrial analogues.

19.6.1 The Galilean moons of Jupiter

The four large (Galilean) satellites of Jupiter are comparable in size to Mercury and our own Moon and represent extremes of planetary processes and morphology (Table 19.4). Each has features preserved from different periods in its history, and each exhibits the effects of quite distinct geomorphic processes. Io, the innermost of the four, is one of the most bizarre planetary bodies in the Solar System (Fig. 19.23). It has a high albedo and a striking reddish-

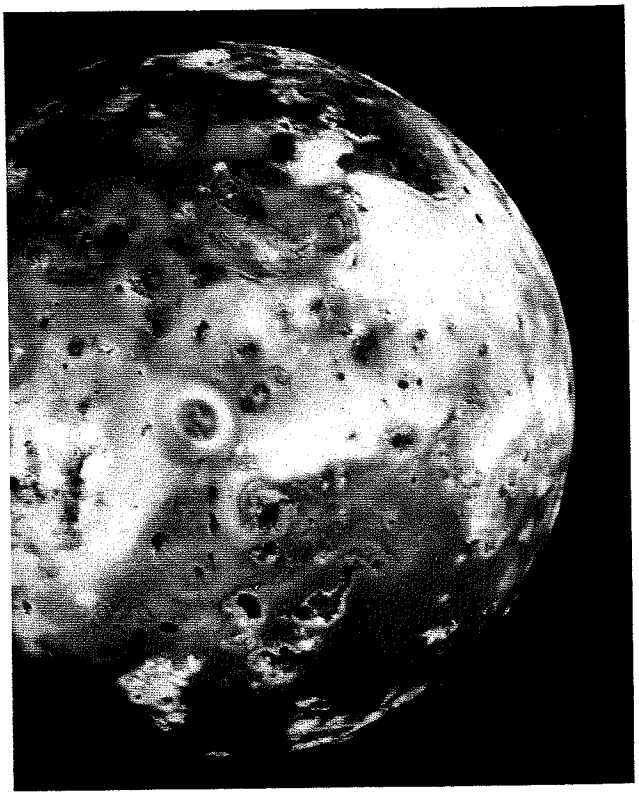

Fig. 19.23 *View of Io taken at a range of 862 200 km. The lack of impact craters on the surface, together with evidence of continuing volcanism, show Io to be an extremely active body. (Voyager 1 image, World Data Center A for Rockets and Satellites.)*

Table 19.4 Properties of the major moons of Jupiter and Saturn

	DIAMETER (km)	DISTANCE (km)	DENSITY(kg m^{-3})
Jovian Moons		(from Jupiter)	
Io	3640	421 600	3530
Europa	3130	670 900	3030
Ganymede	5280	1 070 000	1930
Callisto	4840	1 880 000	1790
Saturnian moons		(from Saturn)	
Tethys	1060	294 700	1210
Dione	1120	377 400	1430
Rhea	1530	527 100	1330
Titan	5150	1 221 900	1880
Iapetus	1460	3 560 800	1160

yellow colour, but quite the most remarkable observation made by the Voyager 1 probe on its transit through the Jovian system was of an active volcano hurling incandescent plumes hundreds of kilometres above its surface (Fig. 19.24). The lack of impact craters on its surface, together with the abundant morphological evidence of widespread volcanism, show Io to be the most active planetary body in the Solar System observed so far. Although some of the energy for this high level of endogenic activity certainly comes from radioactive decay within the planet's rocky interior, additional energy is also supplied from its strong tidal interaction with the giant mass of Jupiter close by. The surface is thus constantly being renewed by fresh eruptions of both silicate-rich and sulphur-rich lavas; any impact craters formed earlier in its history have consequently been obliterated.

Europa, the next satellite out, is, like Io, composed primarily of rock. Its very high albedo and slightly lower density in comparison with Io suggest a 50–100 per cent covering of frost and ice, probably a few kilometres thick, forming its remarkably smooth surface (Fig. 19.25). There are very few impact craters indicating that resurfacing, possibly also promoted by tidal energy derived from the moon's relative proximity to Jupiter, has occurred since the Late Heavy Bombardment (assuming that this event affected this part of the Solar System).

Callisto, the outermost of the Galilean moons, has a much more familiar looking surface dominated by impact craters and multi-ringed basins, presumably formed during the Late Heavy Bombardment and since preserved (Fig. 19.26). Its low density indicates a high ice content, but its low albedo suggests that any surface ice must be heavily contaminated with rock.

Ganymede, lying between the orbits of Callisto and Europa, has the most complex surface of the four Galilean satellites representing an amalgam of heavily cratered Callisto-like terrain and the linear fracture patterns reminiscent of Europa. Its low density indicates a high ice content and its high albedo suggests a 20–60 per cent surface covering of fresh ice. It is conjectured that during the Late Heavy Bombardment the crustal layer of Ganymede was very thin but it subsequently thickened, giving rise to a range of tectonic structures including strike-slip faults and rift zones into which fresh, clean ice was injected.

19.6.2 The moons of Saturn

Of the moons of Saturn, Titan is by far the largest and is exceptional in having a significant atmosphere. It is for this reason that the surface is obscured and consequently its surface morphology is unknown. In spite of their broadly similar density and composition there is no lack of variety in the geomorphology of the other Saturnian satellites imaged by the Voyager fly-bys.

Tethys is the closest to Saturn of the planet's five large moons (diameter greater than 1000 km) (Table 19.4). It has a heavily cratered surface and its most remarkable structure is an enormous impact scar over 400 km across, that is, some 40 per cent of the diameter of the satellite itself. As this feature now shows little vertical relief, it is hypothesized that the interior of Tethys was sufficiently warm and mobile early in its history to accommodate what was obviously an enormous impact without shattering. The burial of some

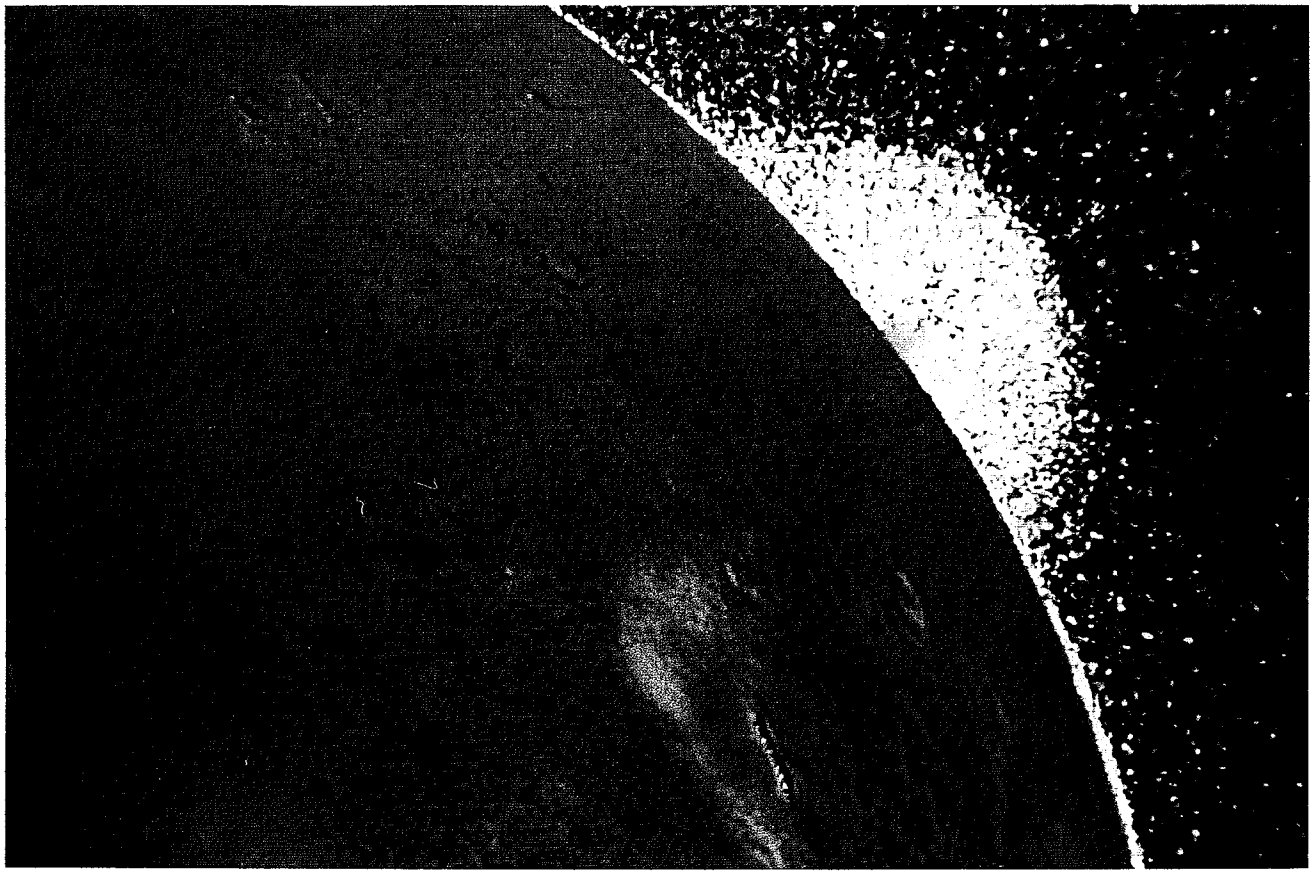

Fig. 19.24 *A volcanic eruption in progress on Io. The brightness of the volcanic plume that can be seen on the horizon rising 100 km from the surface has been greatly increased by computer enhancement. (Voyager 1 image, World Data Center A for Rockets and Satellites.)*

other large craters also indicates a degree of resurfacing on the satellite.

Almost identical in size to Tethys is Dione, orbiting some 80 000 km further out from Saturn. It is the densest moon after Titan and detailed evaluation of its heavily cratered surface suggests that it has been bombarded by two distinct populations of projectiles. The trailing hemisphere, that is, the side facing backward with respect to the direction of its orbital motion around Saturn, has impact craters similar to the lunar highlands and with all the hallmarks of the Late Heavy Bombardment. A second phase of impact cratering with a greater proportion of small projectiles is attributed to

Fig. 19.25 *View of Europa showing a region 600 × 800 km. Particularly noticeable is the network of lineaments on the surface representing low relief ridges and grooves, and contrasts in albedo. These patterns appear to have been caused by stress in the surface crust generated by various possible mechanisms including tidal deformation, global expansion due to dehydration of the interior and freezing of an early ocean. (Voyager 2 image, World Data Center A for Rockets and Satellites.)*

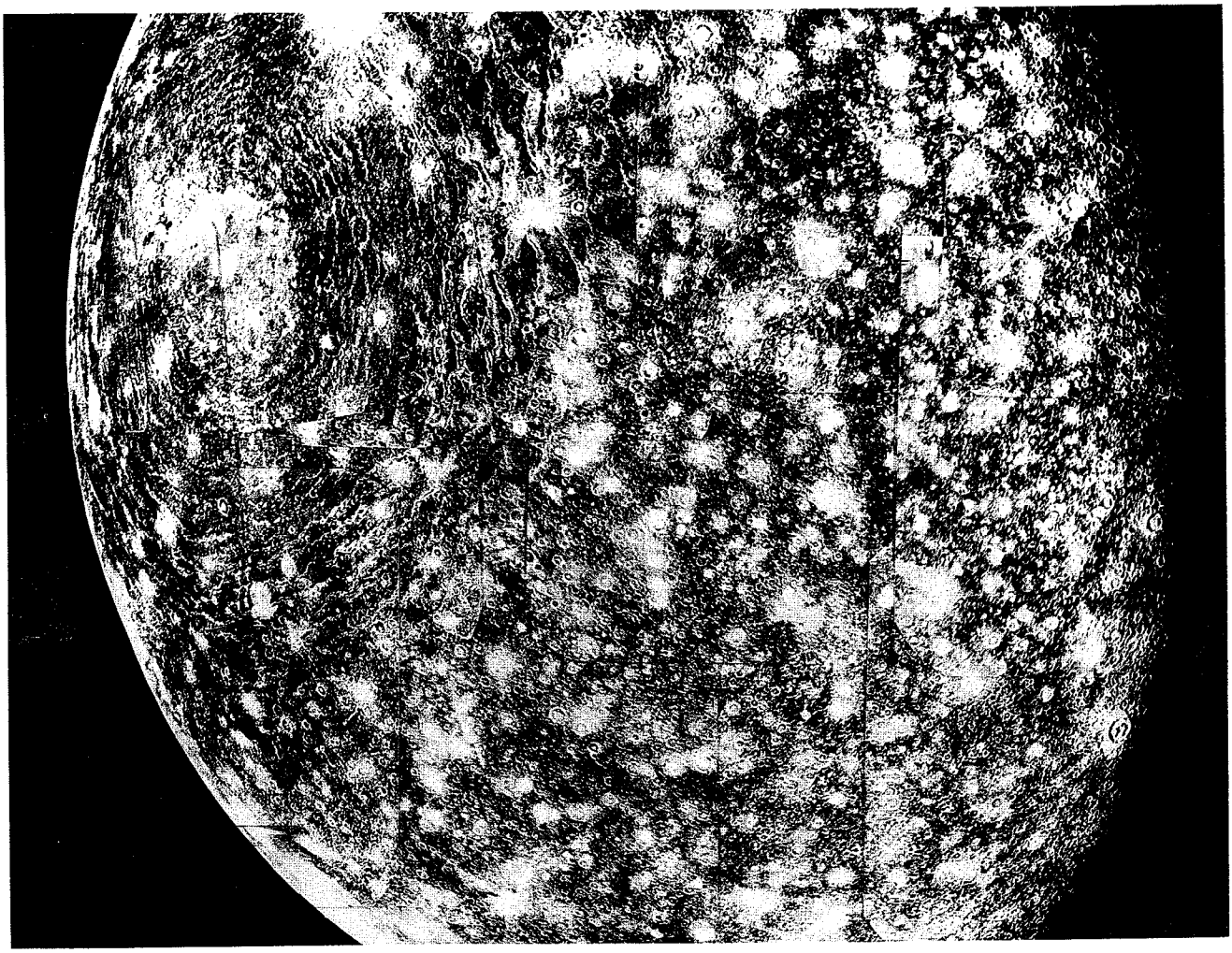

Fig. 19.26 *View of Callisto from a range of 202 000 km. The bright circular region to the upper left of the image is an impact basin about 300 km across. (Voyager 1 mosaic, World Data Center A for Rockets and Satellites.)*

debris generated through collisions within the Saturnian system of moons. This has given rise to a moderate cratering of the plains on Dione formed by resurfacing after the Late Heavy Bombardment. A similar history appears to have been experienced by Rhea which also shows evidence in its distribution of crater sizes for two populations of impacting projectiles. As on Dione, part of the trailing hemisphere shows evidence of resurfacing.

Closely equivalent in size to Rhea is Iapetus, the most distant of Saturn's large moons. It has an incredibly low density of about 1100 kg m^{-3}, and a startling contrast in albedo from around 50 per cent on its trailing hemisphere to an extraordinarily low 3–5 per cent on its leading face; this is possibly a result of dusting by particles originating from Phoebe, the most remote of the Saturnian satellites. An alternative explanation is that the dark material, which has been observed in circular features similar to craters filled by lava flows on the Moon and Mars, was extruded from the interior of the satellite.

19.6.3 The moons of Uranus

Although the images returned from the Voyager probes as they passed through the Jovian and Saturnian systems provided plenty of surprises, the moons of Uranus examined at close quarters by Voyager 2 in January 1986 yielded yet more bizarre surface forms. The 1500 km diameter moon Oberon was seen to have large impact craters with bright rays, and one mountain peak observed was estimated to be some 6 km high. Its comparatively low density of about 1600 kg m^{-3} indicates that it has an icy composition. The slightly smaller moon Ariel with a diameter of about 1200 km has a similarly low density. One of its most remarkable features are canyons which appear to have been flooded by eruptions of ice. These and similar ice-filled valley forms may owe their origin to the extrusion of ice on to the surface as a result of tectonic activity.

The strangest world in the Uranian system is Miranda. Just 480 km in diameter and with a density of only

1200 kg m^{-3}, it is the nearest of the large satellites to Uranus. Its surface is composed of two contrasting types of terrain: one is bright and heavily cratered, whereas the other is darker and lower in elevation and is made up of a series of discrete and apparently unrelated regions of grooved terrain. At present the most widely accepted explanation of this topography is that Miranda suffered a cataclysmic impact early in its history which caused it to break up and then subsequently reaggregate. The now juxtaposed distinctive terrains are thought to have formed as a result of the late accretion of dense fragments which sank slowly through Miranda's outer icy 'mantle' towards its rocky core.

19.6.4 The moons of Neptune

After the startling images acquired of the surfaces of the moons of Jupiter, Saturn and Uranus, it was with great anticipation that researchers awaited the arrival of Voyager 2 at Neptune. In late August 1989 their patience was rewarded by views of a world stranger than anything that had been previously encountered in the epic 12-year journey of Voyager 2. Although initial attention was focused on Neptune itself, interest rapidly shifted to Triton, its largest moon with a diameter of 2700 km. Its fascinatingly complex landscape, which seems to be an assemblage of terrain types previously encountered on other planetary bodies, immediately precipitated a wide range of hypotheses attempting to explain its history.

Predictions prior to the arrival of Voyager 2 were that Triton should be a cold, dead world retaining the scars of the Late Heavy Bombardment. Yet the surface showed much evidence of resurfacing with far less than the expected density of impact craters (Fig. 19.27). Triton, it was thought, had neither the tidal energy of moons like Io, nor the radio-

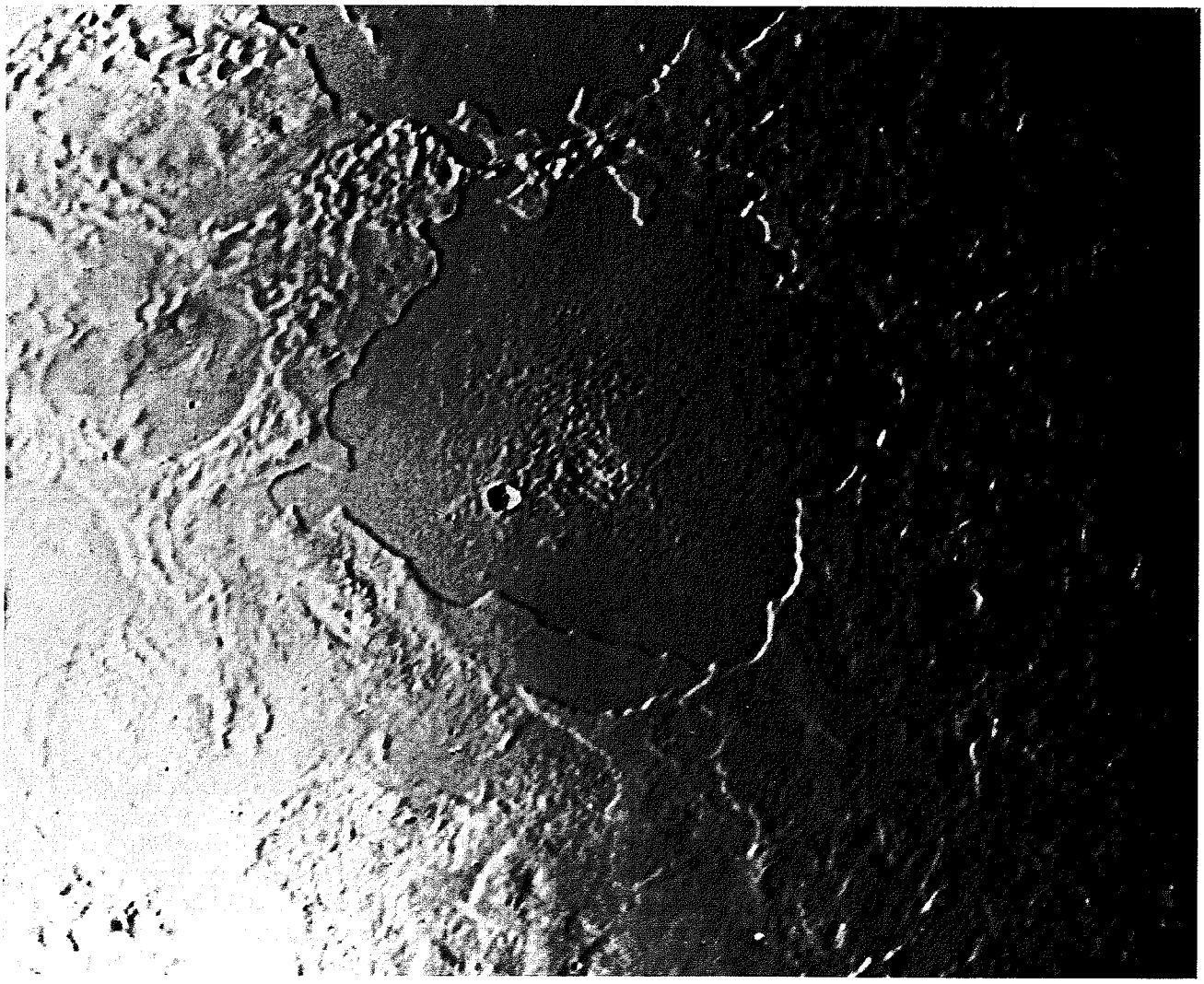

Fig. 19.27 A close-up view about 500 km across of the surface of Triton. The lack of large craters indicates active resurfacing after the Late Heavy Bombardment, but the presence of numerous small craters suggests that generally there has been only a low level of activity over the past 2 Ga. (Voyager 2 mosaic courtesy JPL and NASA.)

active energy of large, rocky planetary bodies to generate sufficient internal heat to have sustained 'volcanic' activity long after its formation. The key to this paradox may lie in Triton's peculiar orbit — it moves opposite to the direction of Neptune's rotation and at an inclination of 21° to the planet's equator. Such an orbit suggests that Triton was captured by Neptune and was pulled into a highly eccentric orbit which alternately took it close to the planet and far away. This type of orbit would have indeed created the kind of tidal energy that drives Io's intense volcanism at the present day. After a few hundred million years the orbit would have become less eccentric, and the reduction in gravitational energy would have caused Triton to cool rapidly. Consequently, the effects of the massive bombardment experienced by all planetary bodies early in the history of the Solar System have been erased from Triton's surface which now only retains evidence of less catastrophic impact events. More recent signs of resurfacing post-dating the Late Heavy Bombardment may be a result of the flowage of methane and nitrogen 'ice' precipitated out of Triton's thin atmosphere.

19.7 Comparative planetary geomorphology

The quantum leap in our knowledge of planetary bodies over the past two decades presents us for the first time with the possibility of making interplanetary comparisons of landforms and the processes that shape them. As we have already emphasized, much of the interpretation of the surface forms of the earth-like planets has been accomplished through analogies with terrestrial landforms. This has served to highlight certain common elements in landform genesis, but for the most part has revealed the considerable contrasts in both the nature and relative intensity of the operation of geomorphic processes throughout the Solar System. The comparative approach to the study of the evolution of planetary surfaces is in its infancy, but it is already possible to suggest some broad generalizations concerning the primary controls of the morphology of the earth-like planetary bodies (Table 19.5).

Until the exploration of the moons of the outer planets, a key variable in the geomorphic evolution of planetary bodies was considered to be size. The Earth has sufficient mass to

Table 19.5 Comparative geomorphology of some earth-like planetary bodies

PLANET/MOON	EXOGENIC PROCESSES	IMPACT CRATERS	VOLCANISM/RESURFACING	TECTONICS
Earth	Active chemical and physical weathering. Mass movement and fluvial, glacial and aeolian erosion and deposition	Very rare–largely obliterated by denudation, volcanism and tectonics	Locally active	Active plate tectonics
Moon	Regolith production by micrometeorite impact and mass movement	Abundant	Locally active early in history	Limited faulting early in history
Venus	Active chemical weathering and probably aeolian action and mass movement	Probably present	Probably active	Uncertain–possibly a form of plate tectonics
Mars	Physical and (limited) chemical weathering. Mass movement and aeolian activity. Phase of fluvial erosion probably early in history.	Fairly abundant	Locally abundant	Major structural lineaments
Mercury	Probably regolith production by micrometeorite impact and mass movement	Abundant	Possibly active early in history	Thrust faulting associated with crustal compression early in history
Io	?	None? presumably obliterated by volcanic resurfacing	Very active	Related to volcanism
Europa	?	Uncommon–presumably obliterated by resurfacing	Resurfacing active early in history?	Linear patterns related to crustal stress
Ganymede	?	Relatively abundant	None	Lineaments with evidence of rifts and strike-slip faulting–form of plate tectonics?
Callisto	Mixing of rock with surface ice (associated with impact cratering?)	Abundant including multi-ringed basins	None	?
Tehtys	?	Abundant	Limited resurfacing	?
Dione	?	Abundant	Limited resurfacing	?
Rhea	?	Abundant	Limited resurfacing	?
Titan	Presence of atmosphere suggests some surface weathering	?	?	?
Iapetus	?	Abundant	Resurfacing by low albedo material	?

retain a significant atmosphere and thereby allow the operation of a wide range of denudational processes. The relatively low surface/volume ratio of the Earth also means that the rate of heat loss from its surface to space has been sufficiently slow to ensure continuing volcanic and tectonic activity promoted by the high temperatures of a molten interior. Smaller bodies, such as the Moon and Mercury, have a higher surface/volume ratio and consequently have experienced a much more rapid rate of cooling than the Earth. A rigid outer crust formed early in their history which was thus able to retain the scars of the Late Heavy Bombardment. Moreover, both the Moon and Mercury are too small, and therefore have insufficient surface gravity, to have prevented the escape of gas molecules and thus retained an atmosphere. Mars is roughly intermediate in size between the Earth and the Moon and Mercury and, as would be expected, it has both an intermediate atmospheric pressure and level of tectonic and volcanic activity. On this basis we would expect Venus to have a level of endogenic activity not very dissimilar to the Earth, since it is of comparative mass.

In broad terms, then, size (or more strictly mass) appears to be a significant factor in controlling the mode of geomorphic development of planetary bodies. This simple relationship, however, breaks down when we turn to the larger satellites of Jupiter and Saturn. In Figure 19.28 most of the larger earth-like planets and moons of the Solar System are plotted in a three-dimensional diagram, the axes of which represent size, composition and state of thermal evolution (that is, the nature and history of tectonic and volcanic activity). The inner planets all have a similar rocky composition, but several of the moons of Saturn are low-density bodies composed predominantly of ice. Even though they are very small in comparison with the Moon and Mercury, these satellites (Tethys, Dione, Rhea and Iapetus) show some evidence of resurfacing after the Late Heavy Bombardment. It seems likely that this activity, in spite of a lack of mass, is a consequence of their icy composition since ice has a far lower melting-point than rock and is therefore capable of producing tectonic activity at much lower temperatures. Hence on our diagram these satellites plot as about as tectonically evolved as the Moon, even though they are much smaller.

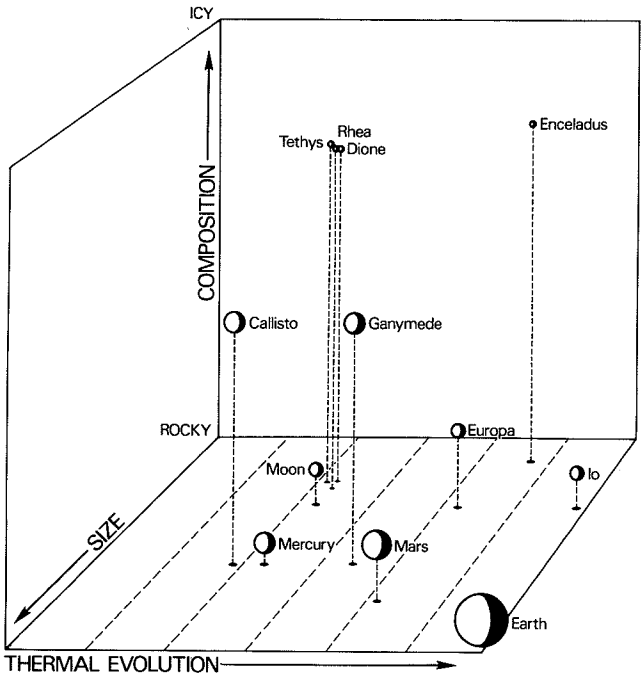

Fig. 19.28 A comparison of major characteristics of some earth-like planets. (Adapted from L. A. Soderblom and T. V. Johnson, (1982) Scientific American ***246****(1), p. 86. Copyright © (1982) by Scientific American, Inc. All rights reserved.)*

Turning to the Galilean moons of Jupiter we appear to have more exceptions to the size rule. These satellites are of the same order of size as the Moon, but they range in their degree of thermal evolution from the highly evolved Io to the poorly evolved Callisto. If we look more carefully, though, we see that the level of thermal evolution of each of the Galilean moons decreases with their increasing distance from Jupiter. This is apparently because Io, the innermost satellite, derives a significant proportion of its internal energy from its tidal interaction with its giant mother planet. This may also apply, albeit to much smaller extent, to Europa.

Perhaps the most remarkable satellite in the Saturnian and Jovian systems is Enceladus, a small moon orbiting close to Saturn. Although it has a diameter of only 500 km and has only 0.1 per cent of the mass of the Moon, it has a complex surface suggesting comparatively recent tectonic activity. Again this is probably associated with the generation of tidal energy due to the close proximity of the large mass of Saturn. Further examples of small planetary bodies with active resurfacing processes are provided by the moons of Uranus.

19.8 Global geomorphology

It is appropriate to conclude this chapter on planetary geomorphology by briefly considering what impact the study of planetary landscapes has had on geomorphology as a whole and, perhaps more importantly, what developments it is likely to precipitate in the future. One obvious contribution has been in the development, and more particularly the use, of remote sensing techniques in landform analysis. Planetary exploration has been founded, the manned Apollo missions notwithstanding, on data collection by unmanned satellites carrying remote sensing equipment. This has prompted the greater application of satellite imagery to the investigation of terrestrial landforms, as exemplified by the production of a landform atlas by NASA researchers and others based on satellite imagery, although there is much

scope for further developments in this field. Global surveys of terrestrial dune systems have now been undertaken, based largely on Landsat imagery and prompted by the need for a comparative database for the interpretation of images of Martian dune systems. A further development has been the space shuttle imaging radar programme which, although so far attaining only a limited geographical coverage, has demonstrated the value of radar techniques in providing images of landforms in regions such as the humid tropics where persistent cloud cover limits the value of conventional Landsat imagery.

A second contribution provided by the exploration of the inner planets has been the stimulation of research on particular geomorphic processes. The realization of the important role played by aeolian processes on Mars, for instance, arising from the identification of vast dune systems and wind-eroded terrain on Pioneer and Viking imagery, has led to a significant growth in laboratory and field studies of terrestrial aeolian activity and landforms.

A third contribution of planetary geomorphology to the study of terrestrial landscapes has been the emphasis placed in the former on catastrophic events. Not only meteorite impact craters but also the formation of features such as the Martian outflow channels seem to be explicable only in terms of the operation of rapidly acting, highly energetic and devastating geomorphic processes. Such an emphasis has led to a re-evaluation of the role of catastrophic processes in shaping the Earth's relief.

Perhaps the most significant stimulus provided by the exploration of planetary landscapes, however, is one which has yet to be fully realized; it is an enlargement of the conceptions of the spatial and temporal scales with which geomorphologists should be concerned. Coupled with major advances in other fields within the earth sciences, such as those represented by plate tectonics and contemporary theories of long-term climatic change, the investigation of planetary landscapes provides us with an exciting new global perspective for geomorphology.

Further reading

Before the space missions of the 1960s and 1970s little was known of the surface features of the earth-like planets, but since 1970 there has been a flood of data from a variety of planetary orbiter and lander missions. There are now hundreds of articles on aspects of planetary geomorphology and only a very small selection is mentioned here. Virtually all of these have been published outside the normal outlets for geomorphic research, the publications *Icarus* and *Journal of Geophysical Research* being particularly useful sources. For a general introduction to planetary geomorphology there is no better starting point than the extensively illustrated book by Greeley (1986).

The results of the Apollo missions to the Moon have appeared in the proceedings of the various lunar science conferences published as supplements of *Geochimica et Cosmochimica Acta*. Burnett (1975) and El-Baz (1975) also provide assessments of the major results of the Apollo programme while Wilhelms (1987) has presented a superbly illustrated survey of lunar geomorphology. Contrasting estimates of cratering rates throughout the history of the Moon are to be found in Guiness and Arvidson (1977) and Neukum and König (1976), while crater morphology is considered by Hale and Grieve (1982), Head (1976a) and Pike (1977). Lunar volcanism is reviewed by Head (1976b), and the origin of lunar rilles and mare ridges is discussed by Lucchitta (1976) and Solomon and Head (1979).

The discussion of Martian geomorphology in this chapter draws extensively from the excellent review by Baker (1981a); other general surveys include the introductory article by Arvidson *et al.* (1978) and the detailed and comprehensively illustrated book by Carr (1981). A large number of papers on various aspects of the geomorphology of Mars are to be found in two supplements of the *Journal of Geophysical Research* (**84**, 7909–8519 (1979), and **87**, 9717–10 305 (1982)).

Impact craters on Mars and their associated layered debris are discussed by Carr *et al.* (1977a) and Mouginis-Mark (1979), while Carr (1976) provides an introduction to the volcanic features on the planet, a treatment which is supplemented by a more detailed discussion in Carr *et al.* (1977b) and a comparison with terrestrial volcanism in Malin (1977). The Valles Marineris structure is considered by Blasius *et al.* (1977), Sleep and Phillips (1979) suggest an isostatic model for the formation of the Tharsis Montes volcanic province, and the broader question of Martian tectonics is tackled by Wise *et al.* (1979). Clark and Van Hart (1981) and Berkley and Drake (1981) present ideas on weathering, and Sharp and Malin (1984) provide an overview of our present knowledge of deposits on the Martian surface based on Viking lander data. Mass movement on Mars is discussed in papers by Lucchitta (1979) on the spectacular landslides of the Valles Marineris and Kochel and Peake (1984) on the morphometry of the debris flows of the fretted terrain.

Aeolian features on Mars have been extensively investigated through analogies with terrestrial forms by Breed (1977), Breed *et al.* (1979) and Ward (1979). Ward *et al.* (1985) provide a comprehensive assessment of the occurrence of aeolian features on the planet, and the processes of wind abrasion are considered in the context of terrestrial aeolian action by Greeley *et al.* (1985). The best overall coverage of planetary aeolian processes, not only for Mars and the Earth but also for Venus, is the book by Greeley and Iversen (1985).

Permafrost on Mars is reviewed by Carr and Schaber (1977) and Lucchitta (1981) draws comparisons between periglacial features on Mars and Earth. The layered depo-

sits of the poles and other problems of the polar terrain are discussed in Cutts *et al.* (1979), while Lucchitta *et al.* (1981) speculate on the role of glacial erosion on Mars and Clifford (1987) assesses the role of melting in generating chaotic terrain and outflow channels.

The enigmatic Martian channels have generated a large literature. A useful starting point is Baker (1981b), while a selection of views concerning the origin of outflow channels include those in Masursky *et al.* (1977), Carr (1979), Komar (1980), Nummedal and Prior (1981) and Cutts and Blasius (1981). The origin and modification of small Martian valleys are discussed by Baker and Partridge (1986) and Brakenridge *et al.* (1985). In view of the wide range of proposed mechanisms of channel formation it is fortunate that there is also a comprehensive overview available (Mars Channel Working Group, 1983). Baker (1985a) looks at the role of fluvial activity on Mars, while Carr (1987) takes a broad look at the role of water in the planet's history.

A useful assessment of the results of the Mariner 10 mission to Mercury is provided by Strom (1979), while the initial results of this project are contained in Murray (1975) and a special issue of *Icarus* (**28**, 429–609 (1976)). The possible gravitational effects of the Sun on the tectonics of Mercury is examined in Burns (1976), while McCauley *et al.* (1981) review the Caloris Basin and Dzurisin (1978) presents a general discussion of the tectonic features of the planet.

The morphology of the Venusian surface as revealed by radar altimetry is discussed by Barsukov *et al.* (1986), Basilevsky and Head (1988) and Head *et al.* (1985). An evaluation of the data collected by the various Soviet Venera landers is provided by Garvin *et al.* (1984), while White (1981) and Nozette and Lewis (1982) speculate on the nature of weathering and erosion. The intriguing question of whether there is a form of plate tectonics operative on Venus is addressed by Brass and Harrison (1982), Head *et al.* (1981) and Solomon and Head (1982), while Head and Wilson (1986) examine the possibilities of volcanic landforms.

Results from the Voyager missions to Jupiter and Saturn have rapidly generated a large literature. Useful surveys of the initial data on the larger satellites are to be found in Soderblom (1980) (Jovian moons), Soderblom and Johnson (1982) (Saturnian moons) and Johnson *et al.* (1987) (Uranian moons), but for a more detailed coverage the book by Greeley (1986) should be consulted.

The broader topic of comparative planetary geomorphology, as well as being addressed by Greeley (1986), is considered from a tectonic perspective by Head and Solomon (1981). Rossbacher and Rhodes (1987) provide an excellent example of the analogies that can be drawn between terrestrial and planetary landforms attributable to catastrophic flooding. It is to the essay by Baker (1985b), however, that readers should turn for a creative, optimistic and thoroughly convincing view of the potential value of this infant research field for geomorphology as a whole.

References

Arvidson, R. E., Binder, A. B. and Jones K. L. (1978) The surface of Mars. *Scientific American* **238**(3), 76–89.

Baker, V. R. (1981a) The geomorphology of Mars. *Progress in Physical Geography* **5**, 473–513.

Baker, V. R. (1981b) *The Channels of Mars*. University of Texas Press, Austin.

Baker, V. R. (1985a) Models of fluvial activity on Mars. In: M. J. Woldenberg (ed.) *Models in Geomorphology*. Allen and Unwin, Boston and London, 287–312.

Baker, V. R. (1985b) Relief forms on planets. In: A. Pitty (ed.) *Themes in Geomorphology*, Croom Helm, London, 245–59.

Baker, V. R. and Partridge, J. B. (1986) Small Martian valleys: Pristine and degraded morphology. *Journal of Geophysical Research* **91**, 3561–72.

Barsukov, V. L. *et al.* (1986) The geology and geomorphology of the Venus surface as revealed by the radar images obtained by Veneras 15 and 16. *Journal of Geophysical Research* **91**, D378–D398.

Basilevsky, A. T. and Head, J. W. III (1988) The geology of Venus. *Annual Review of Earth and Planetary Sciences* **16**, 295–317.

Berkley, J. L. and Drake, M. J. (1981) Weathering on Mars: Antarctic analog studies. *Icarus* **45**, 231–49.

Blasius, K. R., Cutts, J. A., Guest, J. E. and Masursky, H. (1977) Geology of the Valles Marineris, first analysis of imaging from the Viking 1 orbiter primary mission. *Journal of Geophysical Research* **82**, 4067–91.

Brakenridge, G. R., Newsom, H. E. and Baker, V. R. (1985) Ancient hot springs on Mars: origins and paleoenvironmental significance of small Martian valleys. *Geology* **13**, 859–62.

Brass, G. W. and Harrison, C. G. A. (1982) On the possibility of plate tectonics on Venus. *Icarus* **20**, 326–40.

Breed, C. S. (1977) Terrestrial analogs of the Hellespontus dunes, Mars. *Icarus* **20**, 326–40.

Breed, C. S., Grolier, M. J. and McCauley, J. F. (1979) Morphology and distribution of common 'sand' dunes on Mars: comparisons with Earth. *Journal of Geophysical Research* **84**, 8183–204.

Burnett, D. S. (1975) Lunar science: The Lunar legacy. *Reviews of Geophysics and Space Physics* **13**, 13–34.

Burns, J. A. (1976) Consequences of the tidal slowing of Mercury. *Icarus* **28**, 453–8.

Carr, M. H. (1976) The volcanoes of Mars. *Scientific American* **234**(4), 32–43.

Carr, M. H. (1979) Formation of Martian flood features by release of water from confined aquifers. *Journal of Geophysical Research* **84**, 2995–3007.

Carr, M. H. (1981) *The Surface of Mars*. Yale University Press, New Haven, and London.

Carr, M. H. (1987) Water on Mars. *Nature* **326**, 30–5.

Carr, M. H., Crumpler, L. S., Cutts, J. A., Greeley, R., Guest, J. E. and Masursky, H. (1977a) Martian impact craters and emplacement of ejecta by surface flow. *Journal of Geophysical Research* **82**, 4055–65.

Carr, M. H., Greeley, R., Blasius, K. R., Guest, J. E. and Murray, J. B. (1977b) Some Martian volcanic features as viewed from the Viking orbiters. *Journal of Geophysical Research* **82**, 3985–4015.

Carr, M. H. and Schaber, G. G. (1977) Martian permafrost features. *Journal of Geophysical Research* **82**, 4039–54.

Clark, B. C. and Van Hart, D. C. (1981) The salts of Mars. *Icarus* **45**, 370–8.

Clifford, S. M. (1987) Polar basal melting on Mars. *Journal of Geophysical Research* **92**, 9135–52.

Cutts, J.A and Blasius, K.R. (1981) Origin of Martian outflow channels: The eolian hypothesis. *Journal of Geophysical Research* **86**, 5075–102.

Cutts, J. A., Blasius, K. R. and Roberts, W. J. (1979) Evolution of Martian polar landscapes: interplay of long-term variations in perennial ice cover and dust storm intensity. *Journal of Geophysical Research* **84**, 2975–94.

Dzurisin, D. (1978) The tectonic and volcanic history of Mercury as inferred from studies of scarps, troughs and other lineaments. *Journal of Geophysical Research* **83**, 4883–906.

El-Baz, F. (1975) The Moon after Apollo. *Icarus* **25**, 495-537.

Garvin, J. B., Head, J. W., Zuber, M. T. and Helfenstein, P. (1984) Venus: The nature of the surface from Venera panoramas. *Journal of Geophysical Research* **89**, 3381–99.

Greeley, R. (1986) *Planetary Landscapes* (revised edn). Allen and Unwin, London and Boston.

Greeley, R. and Iversen, J. D. (1985) *Wind as a Geological Process*. Cambridge University Press, Cambridge and New York.

Greeley, R., Williams, S. H., White, B. R., Pollack, J. B. and Marshall, J. R. (1985) Wind abrasion on Earth and Mars. In: M. J. Woldenberg (ed.) *Models in Geomorphology*. Allen and Unwin, Boston and London, 373–422.

Guiness, E. A. and Arvidson, R. E. (1977) On the constancy of the lunar cratering flux over the past 3.3×10^9 yr. *Geochimica et Cosmochimica Acta Supplement* **8**, 3475–94.

Hale, W. S. and Grieve, R. A. F. (1982) Volumetric analysis of complex lunar craters: implications for basin ring formation. *Journal of Geophysical Research* **87**, A65–A76.

Head, J. W. III (1976a) The significance of substrate characteristics in determining the morphology and morphometry of lunar craters. *Geochimica et Cosmochimica Acta Supplement* **7**, 2913–30.

Head, J. W. III (1976b) Lunar volcanism in space and time. *Reviews of Geophysics and Space Physics* **14**, 265–300.

Head, J. W. III, Peterfreund, A. R., Garvin, J. B. and Zisk, S. H. (1985) Surface characteristics of Venus derived from Pioneer Venus altimetry, roughness and reflectivity measurements. *Journal of Geophysical Research* **90**, 6873–85.

Head, J. W. III and Solomon, S. C. (1981) Tectonic evolution of the terrestrial planets. *Science* **213**, 62–76.

Head, J. W. III and Wilson, L. (1986) Volcanic processes and landforms on Venus: Theory, predictions and observations. *Journal of Geophysical Research* **91**, 9407–46.

Head, J. W. III, Yuter, S. E. and Solomon, S. C. (1981) Topography of Venus and Earth: A test for the presence of plate tectonics. *American Scientist* **69**, 614–23.

Johnson, T. V., Brown, R. H. and Soderblom, L. A. (1987) The moons of Uranus. *Scientific American* **256**(4), 40–52.

Kochel, R. C. and Peake, R. T. (1984) Quantification of waste morphology in Martian fretted terrain. *Journal of Geophysical Research* **89**, C336–C350.

Komar, P. D. (1980) Modes of sediment transport in channelized water flows with ramifications to the erosion of the martian outflow channels. *Icarus* **42**, 317–29.

Lucchitta, B. K. (1976) Mare ridges and related highland scarps – result of vertical tectonics. *Geochimica et Cosmochimica Acta Supplement* **7**, 2761–82.

Lucchitta, B. K. (1979) Landslides in Valles Marineris, Mars. *Journal of Geophysical Research* **84**, 8097–113.

Lucchitta, B. K. (1981) Mars and Earth: Comparison of cold-climate features. *Icarus* **45**, 264–303.

Lucchitta, B. K., Anderson, D. M. and Shoji, H. (1981) Did ice streams carve Martian outflow channels? *Nature* **290**, 759–63.

Malin, M. C. (1977) Comparison of volcanic features of Elysium (Mars) and Tibesti (Earth) *Geological Society of America Bulletin* **88**, 908–19.

Mars Channel Working Group. (1983) Channels and valleys on Mars. *Geological Society of America Bulletin* **94**, 1035–54.

Masursky, H., Boyce, J. M., Dial, A. L., Schaber, G. G. and Strobell, M. E. (1977) Classification and time of formation of Martian channels based on Viking data. *Journal of Geophysical Research* **82**, 4016–38.

McCauley, J. F., Guest, J. E., Schaber, G. G., Trask, N. J. and Greeley, R. (1981) Stratigraphy of the Caloris basin, Mercury. *Icarus* **47**, 184–202.

Mouginis-Mark, P. J. (1979) Martian fluidized crater morphology: variations with crater size, latitude, altitude and target material. *Journal of Geophysical Research* **84**, 8011–22.

Murray, B. C. (1975) Mercury. *Scientific American* **233**(3), 58–68.

Neukum, G. and König, B. (1976) Dating of individual lunar craters. *Geochimica Cosmochimica Acta Supplement* **7**, 2867–81.

Nozette, S. and Lewis, J. S. (1982) Venus: Chemical weathering of igneous rocks and buffering of atmospheric composition. *Science* **216**, 181–3.

Nummedal, D. and Prior, D. B. (1981) Generation of martian chaos and channels by debris flow. *Icarus* **45**, 77–86.

Pike, R. J. (1977) Apparent depth/apparent diameter relation for lunar craters. *Geochimica et Cosmochimica Acta Supplement* **8**, 3427–36.

Rossbacher, L. A. and Rhodes, D. D. (1987) Planetary analogs for geomorphic features produced by catastrophic flooding. In: L. Mayer and D. Nash (eds) *Catastrophic Flooding*. Allen and Unwin, Boston and London, 289–304.

Sharp, R. P. and Malin, M. C. (1984) Surface geology from Viking landers on Mars: A second look. *Geological Society of America Bulletin* **95**, 1398–412.

Sleep, N. H. and Phillips, R. J. (1979) An isostatic model for the Tharsis province, Mars. *Geophysical Research Letters* **6**, 803–6.

Soderblom, L. A. (1980) The Galilean moons of Jupiter. *Scientific American* **242**(1), 68–83.

Soderblom, L. A. and Johnson, T. V. (1982) The moons of Saturn. *Scientific American* **246**(1), 73–86.

Solomon, S. C. and Head, J. W. III (1979) Vertical movements in mare basins: relation to mare emplacement, basin tectonics and lunar thermal history. *Journal of Geophysical Research* **84**, 1667–82.

Solomon, S. C. and Head, J. W. III (1982) Mechanisms for lithospheric heat transport on Venus: Implications for tectonic style and volcanism. *Journal of Geophysical Research* **87**, 9236–46.

Strom, R. G. (1979) Mercury: A Post-Mariner assessment. *Space Science Reviews* **24**, 3–70.

Ward, A. W. (1979) Yardangs on Mars: evidence of recent wind erosion. *Journal of Geophysical Research* **84**, 8147–66.

Ward, A. W., Doyle, K. B., Helm, P. J., Weisman, M. K. and Witbeck, N. E. (1985) Global map of eolian features on Mars. *Journal of Geophysical Research* **90**, 2038–56.

White, B. R. (1981) Venusian saltation. *Icarus* **46**, 226–32.

Wilhelms, D.E. (1987) The geologic history of the Moon. *United States Geological Survey Professional Paper* **1348**.

Wise, D. U., Golombek, M. P. and McGill, G. E. (1979) Tectonic evolution of Mars. *Journal of Geophysical Research* **84**, 7934–9.